Artificial Visual System for Orientation Detection

by

Jiazhen Ye

A dissertation

submitted to the Graduate School of Science and Engineering for Education

in Partial Fulfillment of the Requirements

for the Degree of

Doctor of Engineering

Supervisor: Prof. Zheng Tang

Associate Supervisors: Assoc. Prof. Shangce Gao

University of Toyama

Gofuku 3190, Toyama-shi, Toyama 930-8555 Japan

2022

(Submitted June 21, 2022)

Acknowledgements

This thesis was completed under the guidance and care of my supervisor, Professor Tang. During the past five years, I have benefited from Professor Tang's kindness and guidance in my thinking, study and work, as well as his unfailing care and attention in my life. During the study period, Professor Tang provided me with good study conditions and a relaxed research atmosphere. From the selection of the topic, the research to the writing of this thesis, from the generation of ideas to the validation of the thesis, all the efforts and hard work of Professor Tang were poured into this thesis. I have been deeply influenced by Professor Tang's strict discipline and generosity, his academic diligence, rigorous attitude, meticulous work spirit, and profound knowledge, all of which have brought me deep respect and benefited me greatly. I would like to take this opportunity to express my deepest respect and sincere gratitude. I would like to express my heartfelt gratitude to Professor Gao for inspiring me to carry out my thesis work smoothly.

Thanks to all the Ph.D.'s and M.S.'s in the research lab. Their diligence and enthusiasm for learning are always a driving force for me to move forward. During the discussions and exchanges with them, I was able to expand my knowledge, and I was motivated to work hard in my studies. With their sincere cooperation and help, I work very smoothly and happily. I would like to thank the teachers at Toyama University and all the students I spent time with, and I received a lot of help from them during my time together. I would like to express my gratitude to all of them.

I would like to give special thanks to my classmates and my colleagues for their care and encouragement during my illness, and to my family and friends. Throughout my years

of study and work, they have given me great support and love in my life. Without their care and support, I would not have been able to complete my studies successfully during my many years of schooling. Such kindness of warm sun, can't be repaid by grass. Here, I would like to say thank you to them.

Abstract

The human visual system is one of the most important component of the nervous system that provides visual perception to person. The research on orientation detection which neurons of the visual cortex response only to a line stimulus in a particular orientation has been carried out for almost 60 years. However, the basic mechanism of orientation detection remains a mystery. In this paper, we first propose a new orientation detection mechanism based on local orientation detective neurons' dendritic computation. We assume that there be orientation detective neurons which response only to a particular orientation locally and these neurons extract local orientation feature based on nonlinear interactions took place on their dendrites. Then, we realize such local orientation detective neurons with dendritic neurons, use them to obtain the local orientation information, and infer the global orientation from these local orientation information. Based on the mechanism, an generalized Artificial Visual System (AVS) for orientation detection and other visual information processing is proposed. In order to prove the effectiveness of our mechanism and the mechanism-based Artificial Visual System (AVS), we conduct a series of experiments which include objects with various sizes and positions. Computer simulation shows that the mechanism can perfectly perform orientation detection independent on their sizes and positions in all experiments. The experimental results are consistent well with the results of most known physiological experiments. Furthermore, we compare the performance of both Artificial Visual System (AVS) and Convolution Neural Network (CNN) on orientation detection and find that Artificial Visual System (AVS) completely beat Convolution Neural Network (CNN) on orientation detection in identification accuracy, noise resistance,

computation cost, learning cost, hardware realization and reasonability.

Secondly, based on the mechanism mentioned above, we use a single-layer McCulloch-Pitts neurons to realize such local orientation detective neurons and show that such a single-layer perceptron artificial visual system (AVS) is also capable of extracting local orientation feature and detecting global orientation by taking the orientation with the largest number of activations of the orientation detective neurons as the global orientation. We perform computer simulations on this single-layer perceptron AVS, and simulation results show that this single-layer perceptron AVS works perfectly for global orientation detection, which is consistent with most of physiological experiments and models.

Finally, as an important category of computational intelligence, meta-heuristic algorithms have always been a popular research interests over recent two decades. Teaching-learning-based optimization (TLBO) is one of nature-inspired meta-heuristic algorithm which is proven to have effectiveness and efficiency in solving complex optimization problems. Although TLBO has remarkable capacity to solve different optimization problems, but the issue of trapping into local optimal is a common drawback of meta-heuristic algorithm, and TLBO is no exception. Thus we use a novel search strategy to improve the performance of TLBO by means of a new selection operation. We select twenty-nine benchmark functions of IEEE CEC2017 to testify the performance of proposed algorithm in terms of effectiveness and robustness. Experimental results exhibit that the proposed algorithm outperforms other state-of-the-art algorithms.

Keywords—visual system, dendritic computation perceptron, single-layer, orientation detection, computational intelligence, teaching-learning-based optimization, search strategy, global optimum.

Contents

List of Figures

List of Tables

Chapter 1

Introduction

In 1981, David Hubel and Torsten Wiesel won the Nobel Prize in Medicine because of their landmark discovery of orientation preference and related works [35, 36]. Based on the remarkable discovery, Hubel and Wiesel found the orientation selective cells in the primary visual cortex (V1) and proposed a simple yet powerful model of how such orientation selectivity could emerge from nonselective thalamocortical inputs [36]. The feedforward model has become a central frame of reference for understanding cortical computation and its underlying mechanisms [27].

Despite 60 years of intense research effort, three basic questions are still unanswered: (1) how, (2) to what degree, and (3) by what mechanisms, does cortical processing contribute to orientation selectivity? In this paper, we first offer a novel quantitative mechanism to provide an explanation for how selectivity for orientation could be produced by a model with circuitry that is based on the anatomy of V1 cortex. We assume that neurons, we call them the local orientation detective neurons, exist in visual nervous system. Each of the local orientation detective neurons receives its own input through photoreceptor and ON-OFF cells from receptive field, picks up selectively an adjacent input, and computes to response only to the orientation from the selected adjacent input. We implement the local orientation detective neuron based on the dendritic neuron model that authors proposed previously [26, 32,48,65,72,82,91] and extend it to several orientation detective neurons that response only to their own particular orientation. Then, we propose four possible schemes to measure the

activations of the local orientation detective neurons: (1) scanning over a two-dimensional inputs of an image, for every inputs, convolving their adjacent inputs with a local orientation detective neuron; (2) scanning over a two-dimensional inputs of an image with a group of the local orientation detective neurons, (3) sliding over a two-dimensional inputs of an image with a small array of a grouped local orientation detective neurons and (4) making a two-dimensional inputs of an image follow their own local orientation detective neurons independently. Since these neurons give the local motion responses that are localized in space; and these neurons' outputs can be taken as evidence about the global orientation, thus we can obtain global orientation directly by measuring the outputs of these local orientation detective neurons. Secondly, based on the mechanism, we propose an generalized Artificial Visual System (AVS) for orientation detection and other visual information processing. To prove the effectiveness of our mechanism and the Artificial Visual System (AVS), we conducted a series of experiments which have a dataset of totally 252,000 images with various sizes, positions at various orientations. Computer simulations show that the mechanism and the mechanism-based Artificial Visual System (AVS) perform the detection of orientation very accurately in all experiments regardless of their sizes and positions. Furthermore, we used a Convolution Neural Network (CNN), trained it to the orientation detection and compared with the Artificial Visual System (AVS). From computer simulations, we found that the Artificial Visual System (AVS) completely beat the Convolution Neural Network (CNN) on orientation detection in identification accuracy, noise resistance, computation cost, learning cost and reasonability.

Based on the mechanism, we also propose a single-layer perceptron AVS for global orientation detection that implements local orientation-selective neurons by a single-layer perceptron of the McCulloch-Pitts neurons. Each neuron is only responsible for detecting a corresponding orientation angle in a two-dimensional local receptive field. Thus, the global orientation detection system can be implemented by a single-layer perceptron AVS. The weights and thresholds of the single-layer perceptron can be designed simply by our

knowledge on perceptron and local orientation-detective neurons. The global orientation of an object can be inferred by the orientation-selective neuron with the largest number of activations. The single-layer perceptron AVS for the global orientation of the object was confirmed by computer simulations on an image dataset. The computer simulation results show that this single-layer perceptron AVS is effective and can make the perfect distinctions on the global orientation of objects regardless of their sizes and positions, which is consistent with most of physiological experiments and models. Furthermore, in order to show the superiority of the single-layer perceptron AVS, we compared the performance of the single-layer perceptron AVS with traditional convolutional neural network (CNN) on global orientation detection tasks and found that the single-layer perceptron AVS completely beats CNN in all aspects including identification accuracy, noise resistance, computational cost, learning cost, hardware implementation, bio-soundness and reasonability.

Furthermore, meta-heuristic algorithm is popularly constructed based on intuitive and experiential rules from diverse phenomenon. It can attain a feasible solution to the optimization problems at an acceptable cost. Generally meta-heuristic algorithm is more able to be applied to real-world complex optimization problems in comparison with classic mathematical optimization algorithm and heuristic algorithm due to its performance and universality, such as traveling salesman problems [13, 20, 90, 94], maximum clique problem [30], wind farm engineering [88], dynamic location routing problem [22], and so on.

Most of meta-heuristic algorithms are inspired by evolution process of nature. Genetic algorithm (GA) mimics the evolutionary process of species which contains crossover operation, selection operation and mutation operation. Ant colony optimization (ACO) is a classical meta-heuristic algorithm that imitates the foraging behavior of ants which deposit pheromone on the ground in order to mark the paths that lead other members of the colony [21]. Artificial bee colony (ABC) algorithm mimics the process of finding a best food source through information interaction among employed bees, onlooker bees and scouts [39, 45]. Artificial immune system (AIS) simulates the immune mechanism of mankind,

therein antigen and antibody are considered as input and output, respectively, and the immune system model consists of antigen-presenting cells layer, major histocompatibility complex layer, Th cell layer, and B cells layer [87].

Although the inspirations of meta-heuristic algorithms are various, recent research [77] shows that most of nature-inspired metaheuristic algorithm could be expressed as in Eq. (1.1):

$$X_{i,d}^{new} = X_{i,d}^{old} + \Sigma_{k=1}^{n} S\left(X_{\alpha,d}^{k}, X_{\beta,d}^{k}\right) \tag{1.1}$$

where $X_{i,d}$ indicates the value of the dth dimension in the ith solution, and X_α and X_β are two certain solutions. $S\left(X_{\alpha,d}^{k}, X_{\beta,d}^{k}\right)$ represents updating unit which is calculated by X_α and X_β, and n denotes the number of updating units. Most updating methods of metaheuristic algorithms can be denoted as in Eq. (1.2).

$$S\left(X_{\alpha,d}, X_{\beta,d}\right) = SF_1() \cdot \left(SF_2() \cdot X_{\alpha,d} - SF_3() \cdot X_{\beta,d}\right) \tag{1.2}$$

where $SF_1()$, $SF_2()$ and $SF_3()$ are scaling factors that used to adjust the scale of difference between X_α and X_β.

Among meta-heuristic algorithms, the teaching-learning- based optimization (TLBO) algorithm is a standard algorithm in the form of updating method described above. It is not hard to observe that TLBO has fast convergence rate, which will be described in the next section. In the meantime, TLBO is also easy to premature and trap into local optimal solutions. In this paper, we utilize a novel search strategy to improve the performance of TLBO and propose a hybrid algorithm named ITLBO. ITLBO exhibits better performance in comparison with other state-of-the-art algorithms based on experimental results. The contribution of this paper can be summarized as follows. First of all, we propose a new hybrid algorithm by incorporating an advanced optimum-based search strategy [93] into the original TLBO, aiming to balance the exploration and exploitation ability of the search.

Secondly, extensive experimental results based on twenty-nine benchmark functions show the superiority of the proposed algorithm, which open the doors to further potential applications on real-world optimization problems. Last but not least, we successfully provide just another example of such hybridization of different meta-heuristic algorithm so long as the embedded strategy is sophisticated, which gives more insights into the key problem of how to design an ensemble optimization algorithm.

Chapter 2

Artificial Visual System Based on Dendritic Computations

2.1 Dendritic Neuron Model

Artificial neural network (ANN) has been a research hotspot in the field of artificial intelligence since the 1980s [34], [30]. ANN is a mathematical model which mimics the information processing mechanism of synaptic connection structure in brain. Until now, artificial neural network has developed hundreds of models, and has a very good performance in such technical fields as medical diagnosis, timeseries forecasting and stock market index prediction [2, 29, 47]. However, all these networks used the traditional McCulloch & Pitts neuron model as their basic computation units [57]. This McCulloch & Pitts model did not take the nonlinear mechanisms of dendrites into account [53]. Meanwhile, recent studies have provided strong circumstantial support for the nonlinear mechanisms of dendrites which play a key role in the overall computation performed by a neuron [1, 4, 5, 14, 16, 54, 73, 76]. Koch, Poggio, and Torre found that in the dendrites of a retinal ganglion cell, if an activated input with inhibitory synapse is closer than an input with excitatory synapse to the cell body, the input with excitatory synapse will be intercepted [49, 50]. Thus, the interaction among the synaptic inputs on dendritic branches can be considered as a logical AND operation [15], and dendritic branch point may sum currents from the dendritic branches, such that its output would be a logical OR on its inputs [6, 17, 33]. It is then conducted to the cell body

(soma), and when it exceeds a threshold, the cell fires to output logical signal 1 to other neurons. Figure 2.1 shows a model that implements an idealized δ cell. If the inhibitory function is described as a logical NOT gate, the operation implemented in Figure 2.1 could be read as:

$$Output = X_1X_2 + \overline{X_3}X_4 + \overline{X_5}X_6X_2 \tag{2.1}$$

where X_1, X_2, X_4 and X_6 denote excitatory inputs and X_3 and X_5 represent inhibitory inputs. Because each input is either logical 0 or 1, the output of the cell body (soma) becomes 1 when and only when $X_1 = 1$ and $X_2 = 1$, or $X_3 = 0$ and $X_4 = 1$ or $X_5 = 0$ and $X_6 = 1$ and $X_2 = 1$. Furthermore, γ cell receives inputs from excitatory and inhibitory synapses distributed from the tip to the cell body (soma) as shown in Figure 2.1b, thus reading,

$$Output = \overline{X_1}X_2X_3 \tag{2.2}$$

Several experimental examples such as motion direction selectivity of retinal ganglion cells in the visual system [80] and coincidence detection in the auditory system [70] have provided strong circumstantial support to Koch's model [49]. By taking nonlinearity of synapses and nonlinear interaction among these synapses into consideration, authors proposed a learnable dendritic neuron model (DNM) [25, 38, 49, 79, 83]. DNM was successfully applied to many burning questions, such as liver disorders analysis, breast cancer classification, financial time series prediction [41, 71, 95].

2.2 Local Orientation Detection Neuron

In this section, we describe the structure of DNM in detail for orientation detection. For simplicity, we only consider the composition of four neurons for orientation detection. Usually, the receptive field can be divided into two-dimensional $M \times N$ regions. Each region

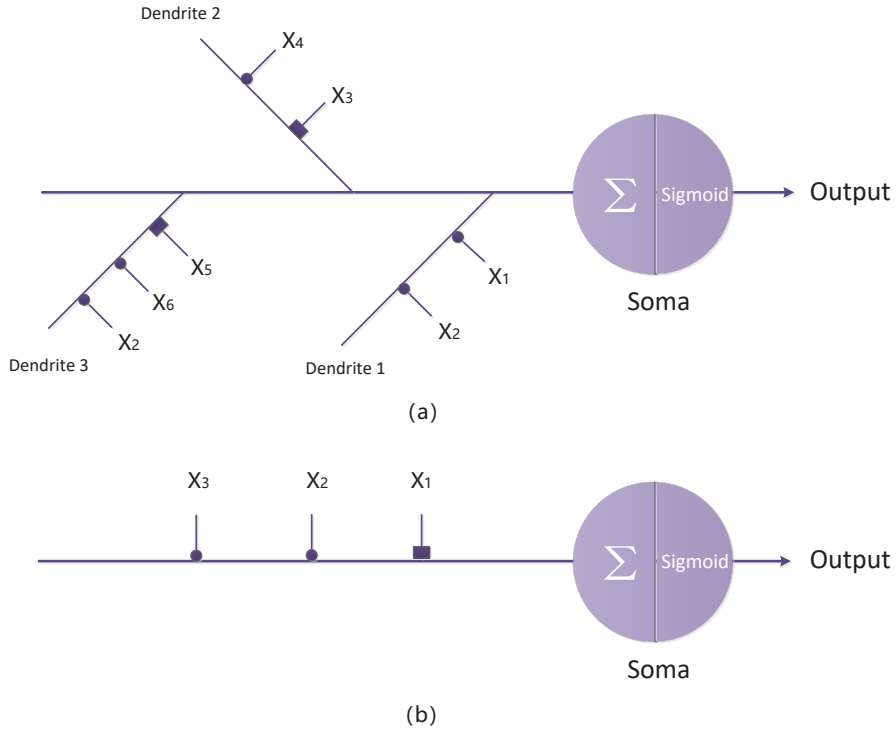

Figure 2.1: Structure of the dendritic neuron model with inhibitory input (■) and excitatory inputs (•). (**a**) δ cell and (**b**) γ cell.

corresponds to a minimal visible region. For simplicity, we consider a binary image. When light falls on a region, the electrical signal, for example, 1 is transferred through its photoreceptor and ON-OFF response cells to ganglion cells and the ganglion cells perform various visual information processing [46]. Of course, by introducing horizontal cell, gray scale images and color images can also be treated easily. Here, we assume that there are simple ganglion neurons that can detect the specific orientation of a line. The input signal can be expressed by $X_{i,j}$, where i and j correspond to position at the two-dimensional receptive field. Thus, for an input signal $X_{i,j}$, if we use the local orientation detective neurons and consider eight regions adjacent to $X_{i,j}$ only, we can implement four neurons by picking up selectively a particular region in that directions. Figure2.2 shows an idealized γ cell for 0 degree orientation detection. What we need to consider is only the $X_{i,j}$, $X_{i-1,j}$ and $X_{i+1,j}$. If and only if $X_{i,j}$, $X_{i-1,j}$ and $X_{i+1,j}$ are all equal to 1, the γ neuron is activated and the

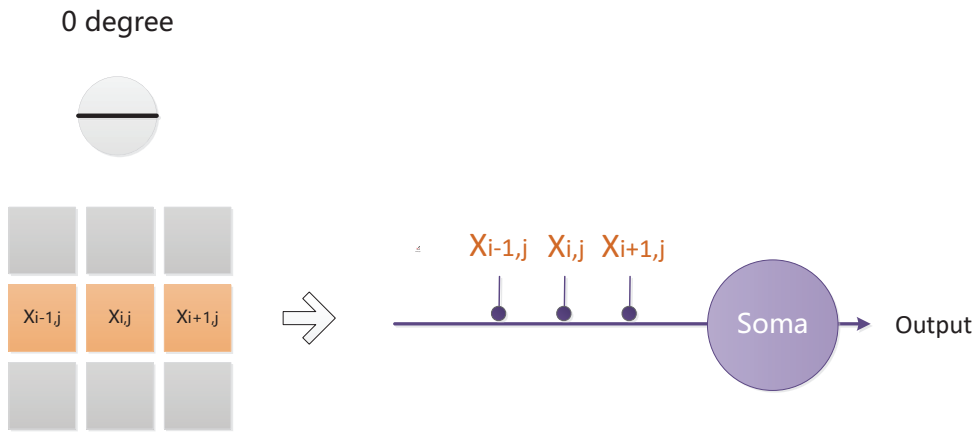

Figure 2.2: A local planar orientation-detective neuron with γ cell for 0 degrees.

output of the soma is equal to 1. Similarly, the detective neurons in other orientations can also be implemented. Four structures of orientation detection neurons can be described in detail as Figure2.3. For example, the 45 degree detective neuron at i, j has different input signals from adjacent inputs $X_{i-1,j+1}$ and $X_{i+1,j-1}$ besides $X_{i,j}$, the inputs to 90 degree detective (vertical detection) neuron at i, j comes from $X_{i,j-1}$ and $X_{i,j+1}$ besides $X_{i,j}$, and the inputs to 135 degree detective neuron at (i, j) is certainly set to $X_{i-1,j-1}$, $X_{i,j}$ and $X_{i+1,j+1}$. Therefore, we can ensure that all orientation detective neurons can be realized by γ-like cells. On account of the size of window (pixel matrix) we chose is 3×3, so we can only select these four orientations. If the size of window increases, more orientations can be detected.

2.3 GLOBAL ORIENTATION DETECTION

As mentioned above, the local orientation detective neurons in the visual system response by performing an interaction of the effect of light falling on their receptive field, for example a local orientation detective neuron extracts a simple one orientation information at one position in the visual field by interacting the input of the position from photoreceptor and ON-OFF response cells with its neighboring inputs. Here, we assume that the information of

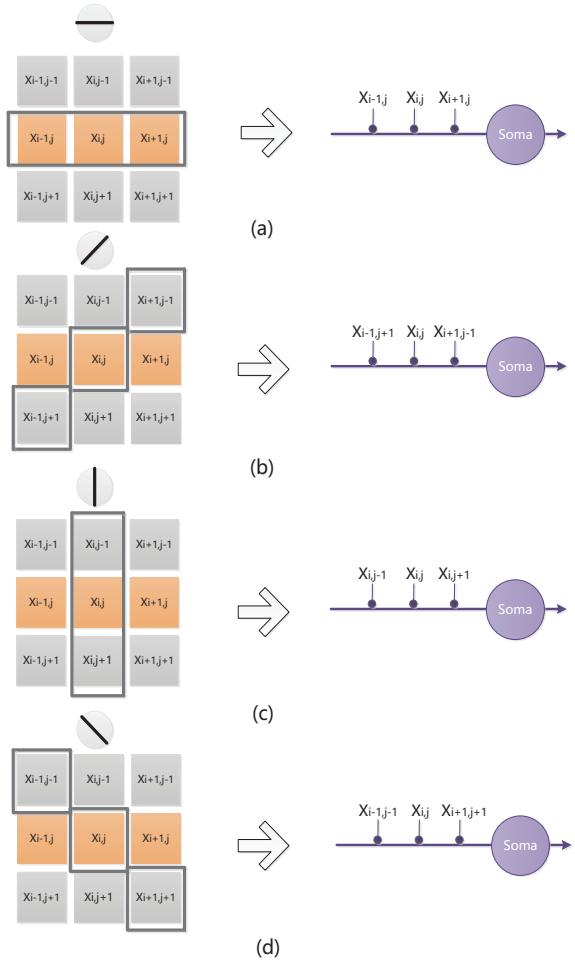

Figure 2.3: The local planar orientation-detective neurons. (**a**) 0 degree, (**b**) 45 degree, (**c**) 90 degree and (**d**) 135 degree neurons.

the local orientation can be used for judging global orientation. Thus, we can just measure the strength of activities of the all local orientation detective neurons over the receptive field (for example, the number of the fired neurons) and derive a judgement of orientation by summing the neurons' outputs in different orientations. In order to measure the strength of activities of the local orientation detective neurons for a two-dimensional receptive field $(M \times N)$, we have four possible schemes:

(1) One Neuron Scheme: assume that there be only one local orientation detective retinal ganglion neuron that scans the every position (i, j) for $i = 1, 2, \ldots, M$ and $j = 1, 2, \ldots, N$

over the two-dimensional receptive field ($M \times N$), and at every position, scans two adjacent positions at one direction to detect the local orientation of the positions;

(2) Multi-Neurons Scheme: we assume, for simplicity, that there be four local orientation detective retinal ganglion neurons that scan every position (i, j) for $i = 1, 2, \ldots, M$ and $j = 1, 2, \ldots, N$ over the two-dimensional receptive field ($M \times N$), and yield the local orientation of the positions;

(3) Neuron-Array Scheme: we assume, for simplicity, that there be four local orientation detective retinal ganglion neurons that are arrayed in $M \times N$ ($m < M$, and $n < N$), that are slid over the two-dimensional receptive field ($M \times N$) without overlapping, and yield the local orientation of the positions;

(4) Full-Neurons Scheme: we assume that every photoreceptor input corresponding to the position (i, j) of a two-dimensional receptive field ($M \times N$) have their own local orientation detective retinal ganglion neurons. That is to say that there are $M \times N \times 4$ local orientation detective retinal ganglion neurons.

Thus, within local receptive field, the local orientation detective neurons can extract elementary local orientation information. The local orientation information is then used to judge global orientation. In order to help the understanding of the mechanism with which the system performs orientation detection, we use a simple two dimensional (5×5) image of a bar in 45 degree as shown in Figure2.4. Without loss of generality, we use the four-neuron scheme in which the four local orientation detective retinal ganglion neurons scan the every position from (1, 1) to (5, 5) over the two-dimensional receptive field (5×5), and yield the local orientation of the positions.

As shown in Figure 2.4, only the 45 degree neuron fires at (3, 3) and (4, 4). The 0 degree neuron, 45 degree neuron and 90 degree neuron fire simultaneously at (3, 4) and (4, 3). The number of the firing neurons in different orientations, 4 for 45 degree, 2 for 0 degree, and 2 for 90 degree can be measured, thus resulting in a judgement of a global 45 degree orientation.

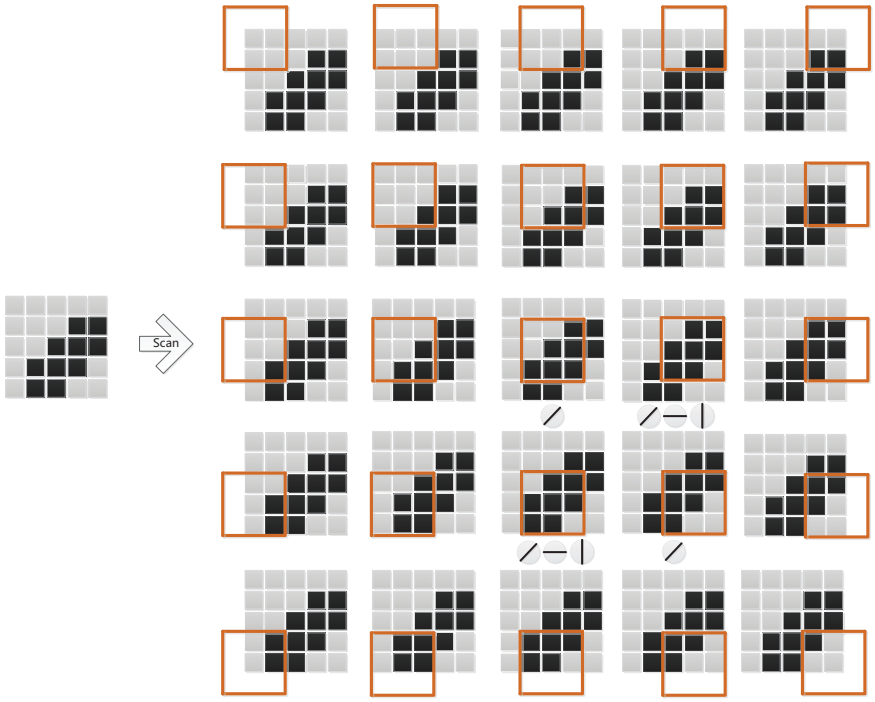

Figure 2.4: Diagram of the judgment of global planar orientation detection by the local planar orientation-detective neurons.

In all the above experiments, because we detected the orientation of only one target object, we scanned the entire image to obtain the local orientation information of each position including the orientation information of the target object, thereby inferring the global orientation of the object. In fact, for a multi-object orientation problem, because we know the local orientation information of each position, we can extract the local orientation information of each target object, from which we can infer the global orientation information of each target object.

2.4 Artificial Visual System (AVS)

The visual system comprises the sensory organ (the eyes), the connecting pathways through to the visual cortex and other parts of central nervous system. As mentioned above, in the

visual system, the local visual feature detective neurons such as local orientation detective neurons can extract elementary local visual feature such as local orientation information. These features are then combined by the subsequent layers in order to detect higher-order feature, for example, the global orientation of an object. Based on the mechanism, we develop an generalized artificial visual system (AVS) as shown in Figure 2.5. Neurons in layer 1 (called the local feature detective neuron (LFDN) layer), such as local orientation detective neurons, extract elementary local visual feature, for example, the local orientation information. These features are then sent the subsequent layers (called global feature detective neuron (GFDN) layers) in order to detect higher-order feature, for example, the global orientation of an object. Neurons in layers can be just simply the summation of the outputs of neurons from layer 1, for example, for the orientation detection, the motion direction detection, the motion speed detection and the perception of the binocular vision; or a one layer even a multi-layer network, for example, for pattern recognition. It is worth noting that the Artificial Visual System (AVS) is a feedforward neural network, and any feedforward neural network can be trained by the error back-propagation method. The difference between the Artificial Visual System (AVS) and traditional multi-layer neural networks as well as convolutional neural networks is that the local feature detective neurons (LFDN) in layer 1 of the Artificial Visual System (AVS) can be designed in advance according to our prior knowledge of real visual system, for example how many neurons and what kind of neurons are needed, and furthermore they do not need to learn in most cases. Even if learning is needed, learning of the Artificial Visual System (AVS) can start from a very good initial value, which can makes learning more efficient and faster.

2.5 Experiment

In order to prove the effectiveness of our proposed mechanism, we randomly generated a large number of different 32×32-pixel images for learning and testing. We scanned every pixels of the two-dimensional images by a 3×3 window, used four orientation detection reti-

nal ganglion neurons to extract the local orientation information of pixels in each window, and made a judgement of the global orientation information based on the local orientation information. First, we chose four bars in three different orientations to test proposed mechanism. The first two bars were at 135 degree angles and had different length-width ratios, while the remaining two bars were horizontal and vertical, respectively. In all computer simulations, we scanned with a 3×3 window and step size was set to 1. Each data of the scanning was transferred to four orientation detection neurons during the scanning procedure, and we counted when the corresponding neurons fired. Experimental results are shown in Figures 2.6–2.9. We set the excited neurons to 1 and inhibited neurons to 0. We used a simple function diagram to represent the output process of the four neurons and the types of detective neuron were labeled in the graph. Finally, we recorded the total number of activations and picked up the maximum of them. Here, the activations of the four kinds of neurons are represented. The horizontal coordinate is the serial number of the corresponding scanning window, and the vertical coordinate is whether the neurons are activated or not. The number of activations is given and the orange box is the maximum value, which is our final judgment for the orientation. From Figure 2.6, we can see that the neurons for angle 0°, 45°, 90° and 135° fire 38, 0, 39 and 74. Thus, 135° orientation can be detected.

Similarly, 135°, horizontal (0°) and vertical (90°) can also be inferred from Figures 2.7–2.9. Finally, we selected seven standard rectangles in 90° with different length-width ratios, and then used a bar chart to show the activation rates of each rectangle, The bar chart of experiments are expressed as Figure 2.10, where the X-axis denotes the length-width ratios and y-axis represents activation rates of four neurons where the length of the bar was fixed at 30-pixel. According to this experiment, we can find that the activation rate is decreased by the decrease of length-width ratios. The closer the rectangle is to a square, the more difficult it is to identify the orientation of the rectangle. For a square, with the length-width (1:1), the rates of neuron for 0° and neuron for 90° are same because even for

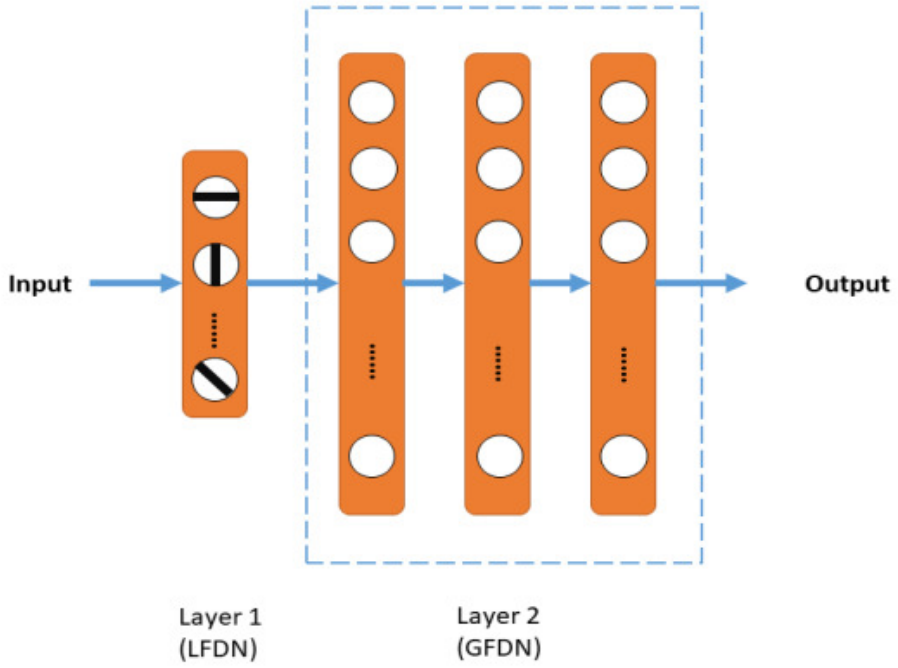

Figure 2.5: A generalized artificial visual system (AVS) with a local feature-detective neuron (LFDN) layer and one or many global feature-detective neuron (GFDN) layers.

the human can't distinguish a square in 0° or 90°. When the length-width becomes to 1:2, neuron for 0° orientation fires most, thus inferring to 0° orientation detection. This hints that the proposed mechanism may be very close to the orientation detection mechanism of the real visual system. From all of these computer experiments, we find that the proposed mechanism and the mechanism-based systems can accurately detect the orientations of objects with different positions, length-width ratios and sizes. Therefore, we can conclude that the proposed mechanism is not only highly accurate in detecting objects in a specific orientation, but also hints that our hypothesis about the orientation detective neurons and the global orientation inferring system is possibly correct.

In order to compare the orientation detective performance of the artificial visual system (AVS) with other methods, we selected convolutional neural networks (CNNs) because they are widely applied with great success to the detection, segmentation and recognition of objects in images. The convolutional neural network (CNNs) used in our experiments

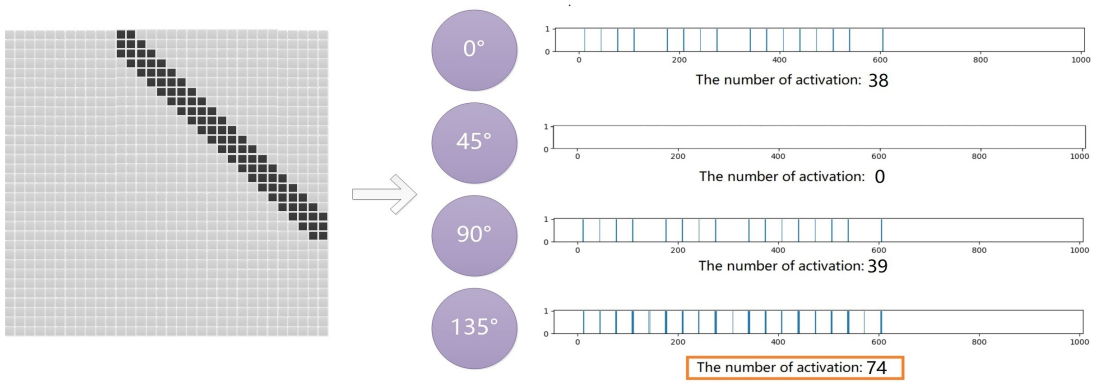

Figure 2.6: Computer experiment on the mechanism for detecting a 135° bar with a width of 3.

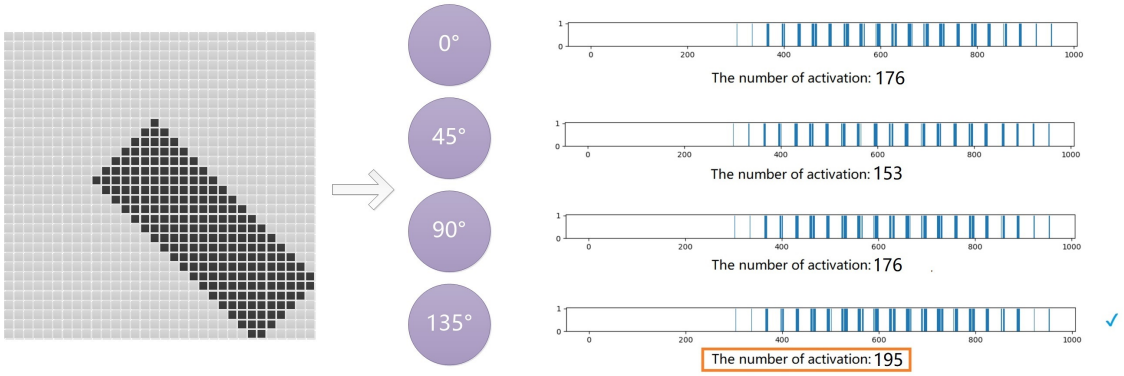

Figure 2.7: Computer experiment on the mechanism for detecting a 135° bar with a width of 7.

comprises 7 layers: (1) Convolutional layer with 30 feature maps connected to a 3×3 neighborhood in the input; (2) ReLu layer; (3) Pooling layer with 2×2 maximum pooling; (4) Affin layer with a full net from 1024 to 720; (5) ReLu layer; (6) Affin layer with a full net from 720 to 4 and (7) Softmax layer. The input was a 32×32 pixel image. The data used to train and test the system was 15000 and 5000, respectively. The sizes of object were from 3 pixels to 100 pixels. Learning was performed by back-propagation under Adam optimizer. The identification accuracy of both CNN and AVS is summarized in Table2.1. As expected, CNN learned the orientation detection very well and reached 99.85% identification accuracy. That is to say that without noises, CNN did not so bad comparing to AVS' 100% accuracy. But, even if only a pixel noise was added, CNN's identification accuracy dropped

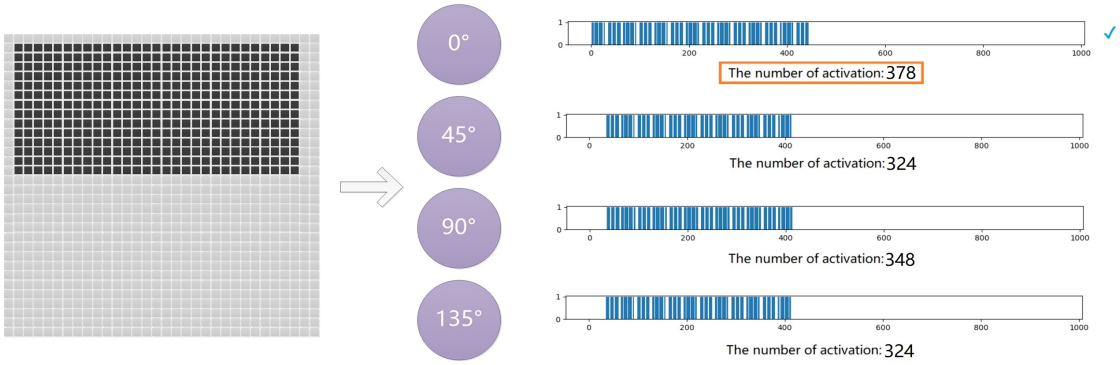

Figure 2.8: Computer experiment on the mechanism for detecting a horizontal (0°) bar.

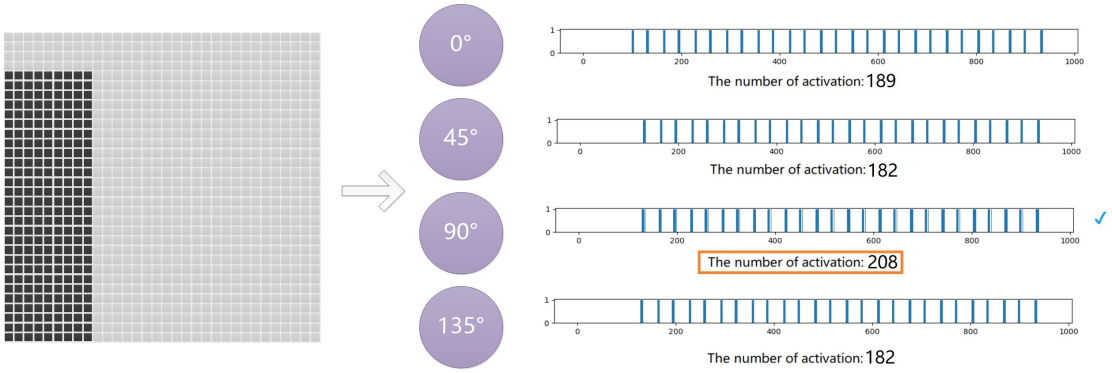

Figure 2.9: Computer experiment on the mechanism for detecting a vertical (90°) bar.

from 99.85% to 97.89% immediately. As the number of noises increased to 150, CNN's identification accuracy would drop dramatically even lower than 30%. In contrary, AVS could always maintain 100% identification accuracy, showing superior noise resistance.

Table 2.1: Comparison of identification accuracy between CNN and AVS.

Noises	**0 Noise**	**1 Noise**	**5 Noises**	**10 Noises**	**25 Noises**	**50 Noises**	**100 Noises**	**150 Noises**
CNN	99.85%	97.89%	59.28%	51.42%	38.04%	35.42%	30.68%	29.38%
AVS	100%	100%	100%	100%	100%	100%	100%	100%

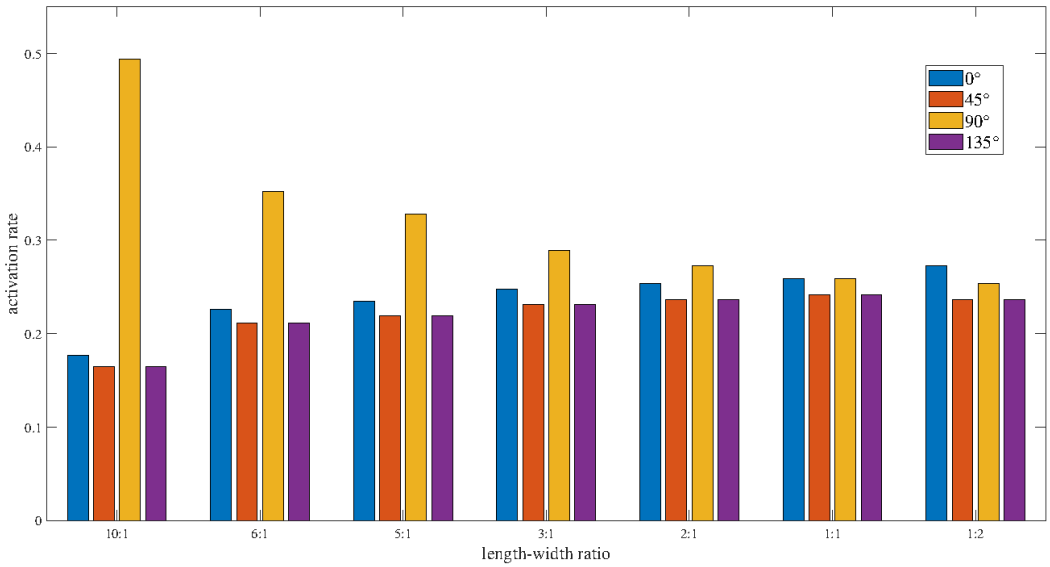

Figure 2.10: The activation of four neurons for a 90° bar with different length–width ratios.

2.6 Conclusion

In this chapter, we offered a novel quantitative mechanism to provide an explanation for how selectivity for orientation could be produced by a model with circuitry that is based on the anatomy of V1 cortex. We assumed that neurons, we call them the local orientation detective neurons, exist in visual nervous system. Each of the local orientation detective neurons receives its own input through photoreceptor and ON-OFF cells from receptive field, picks up selectively an adjacent input, and computes to response only to the orientation from the selected adjacent input. We implemented the local orientation detective neuron based on the dendritic neuron model that authors proposed previously and extend it to several orientation detective neurons that response only to their own particular orientation. Then, we proposed four possible schemes to measure the activations of the local orientation detective neurons: (1) scanning over a two-dimensional inputs of an image, for every inputs, convolving their adjacent inputs with a local orientation detective neuron; (2) scanning over a two-dimensional inputs of an image with a group of the local orientation detective neurons, (3) sliding over a two-dimensional inputs of an image with a small array

of a grouped local orientation detective neurons and (4) making a two-dimensional inputs of an image follow their own local orientation detective neurons independently. Since these neurons give the local motion responses that are localized in space; and these neurons' outputs can be taken as evidence about the global orientation, thus we can obtain global orientation directly by measuring the outputs of these local orientation detective neurons. Secondly, based on the mechanism, we proposed an Artificial Visual System (AVS) for orientation detection and other visual information processing. To prove the effectiveness of our mechanism and the Artificial Visual System (AVS), we conducted a series of experiments which have a dataset of totally 252,000 images with various sizes, positions at various orientations. Computer simulations showed that the mechanism and the mechanism-based Artificial Visual System (AVS) performed the detection of orientation very accurately in all experiments regardless of their sizes and positions. Furthermore, we used a Convolution Neural Network (CNN), trained it to the orientation detection and compared with the Artificial Visual System (AVS). From computer simulations, we found that the Artificial Visual System (AVS) completely beat the Convolution Neural Network (CNN) on orientation detection in identification accuracy, noise resistance, computation cost, learning cost and reasonability.

Chapter 3

Artificail Visual System Based on Single-Layer percetron

3.1 Single-Layer Perceptron

McCulloch-Pitts artificial neuron model was proposed in the 1940s [57]. It is a simple simulation of biological nerve cells. The structure of the McCulloch-Pitts model is shown in Figure 3.1(a). In this model, the neuron receives input signals x_1, x_2, ...,x_n from other neurons. The importance of these input signals is usually represented by the weights of the connections between neurons, w_1, w_2, ...,w_n. The neuron multiplies the received input values with the corresponding weights, sums them to get value $\sum_{i=1}^{n} w_i x_i$, and compares it with a threshold. When the sum exceeds the threshold θ, the neuron fires to output y=1; otherwise, y=0 When several such neurons are combined into a system, as shown in Figure 3.1(b), we call it a perceptron, or a single-layer perceptron, which consists of a single layer of the McCulloch-Pitts neurons connected to a set of inputs from other neurons with their own weights [68].

3.2 Local Orientation-selective Neuron

In this subsection, we use the single-layer perceptron to realize the local orientation-selective neurons. We assume there are many simple neurons with orientation detection function, and each neuron is only responsible for detecting a specific orientation in a small area, the local

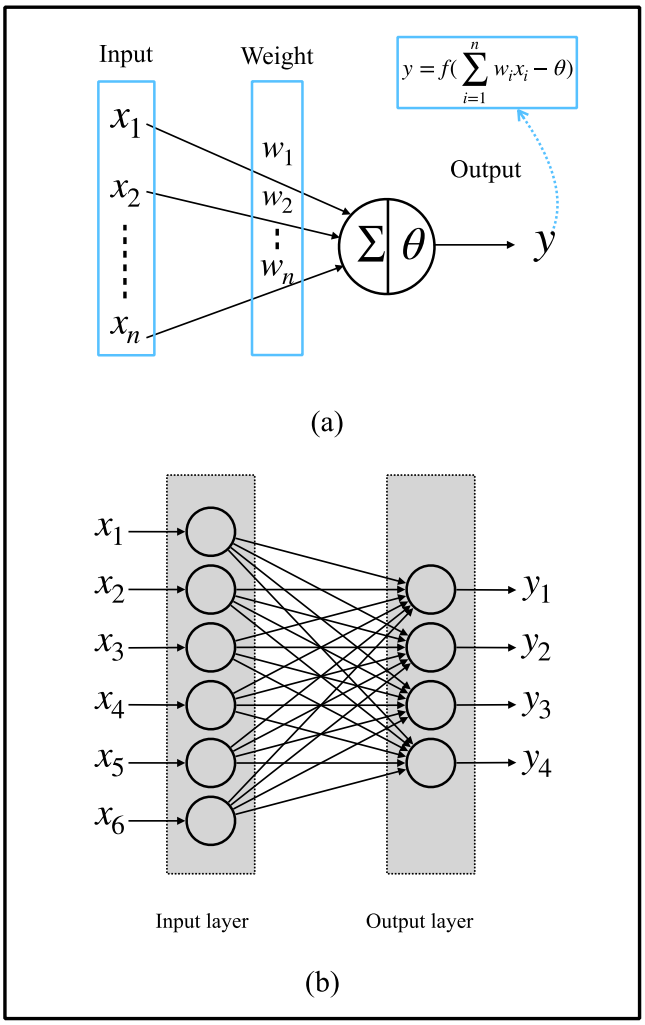

Figure 3.1: The structure of the Single-Layer Perceptron (a) McCulloch-Pitts neuron model, (b) a single-layer perceptron.

receptive field of the whole visual field. For simplicity, we consider a 3×2 local receptive field. There are 4 possible orientation angles of 0°, 45°, 90°, and 135° that can be detected in such a local receptive field. Using four McCulloch-Pitts neurons, we can implement four types of orientation-selective neurons that can detect two-dimensional objects with orientation angles of 0°, 45°, 90°, and 135°, respectively.

In real visual system, the primary visual information transmission pathway is the photoreceptor → bipolar cell → ganglion cell → LGN → primary visual cortex [44]. Considering a two-dimensional visual field, or the receptive field, we assume that the two-dimensional

visual field or the receptive field can be divided into $M \times N$ regions. Each region corresponds to the smallest area that can be visually distinguished. When light falls on a region, a corresponding photoreceptor or a bunch of photoreceptors convert light signals into electrical signals, and then the electrical signals are transmitted to ON-OFF response bipolar cells. To simplify the neural computation, we only use the ON-response mechanism, and thus if a photoreceptor receives light, its corresponding ON-response bipolar cell outputs 1; otherwise, 0. For simplicity, we connect photoreceptors directly to orientation-selective ganglion neurons. Different types of orientation-selective ganglion neurons accept corresponding signals from corresponding ON-response bipolar cell or photoreceptor. Taking x_5 as the reference point, we can obtain the corresponding connections of four types of orientation-selective neurons in a local receptive field with 6 (3×2) regions as shown in Figure 3.2.

From Figure 3.2, we can know that the size of a local receptive field is set as 3×2 and the orientation-selective neurons respond to two inputs. In the 3×2 local receptive field, the input signals are from x_1 to x_6, where the point x_5 is the reference point. Thus, 0°-selective neuron only responds to x_5 and x_6, 45°-selective neuron only responds to x_3 and x_5, 90°-selective neuron only responses to x_2 and x_5, and 135°-selective neuron only responses to x_1 and x_5. Because a photoreceptor receiving light outputs 1; otherwise, 0, and weights (from w_1 to w_6) are all set to 1, and only when two inputs from photoreceptors are 1 simultaneously, this neuron is fired. Thus we can set the threshold as 1.5 and the activation function as a step Eq. (3.1):

$$y = \begin{cases} 1, x_i w_i + x_j w_j \geq 1.5 \\ 0, x_i w_i + x_j w_j < 1.5 \end{cases} \tag{3.1}$$

where x_i and x_j represent the two effective inputs, w_i and w_j are the corresponding weights.

The effective input information of different orientation-selective neurons is different. So,

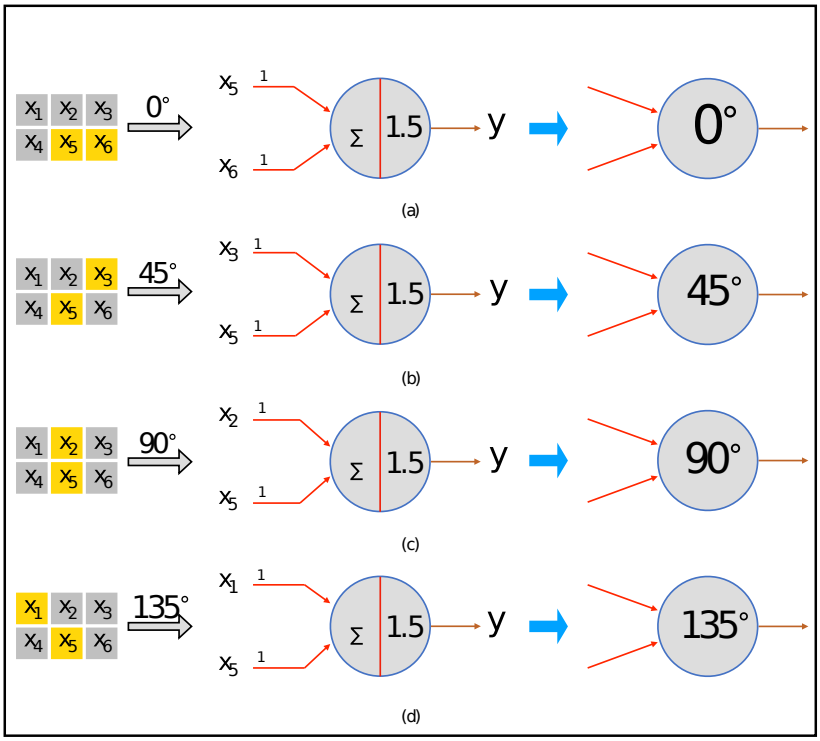

Figure 3.2: The perceptrons for the four types of orientation-selective neurons in a local receptive field. (a) -selective neuron, (b) -selective neuron, (c) -selective neuron and (d) -selective neuron.

we let each corresponding region connect to four different orientation-selective neurons. An example of the connections between photoreceptors and four different orientation-selective neurons in a local receptive field is shown in Figure 3.3. As shown in Figure 3.3(a), for a 3×2 local receptive field, only a region, the reference region is connected to all orientation-detective neurons, and the other four photoreceptors are connected to four corresponding orientation-selective neurons, respectively. Different orientation-selective neurons focus on different outputs of photoreceptors and accept corresponding orientational information. If we describe the neural connection in a local receptive field as a perceptron form, the perceptron AVS can be shown as Figure 3.3(b).

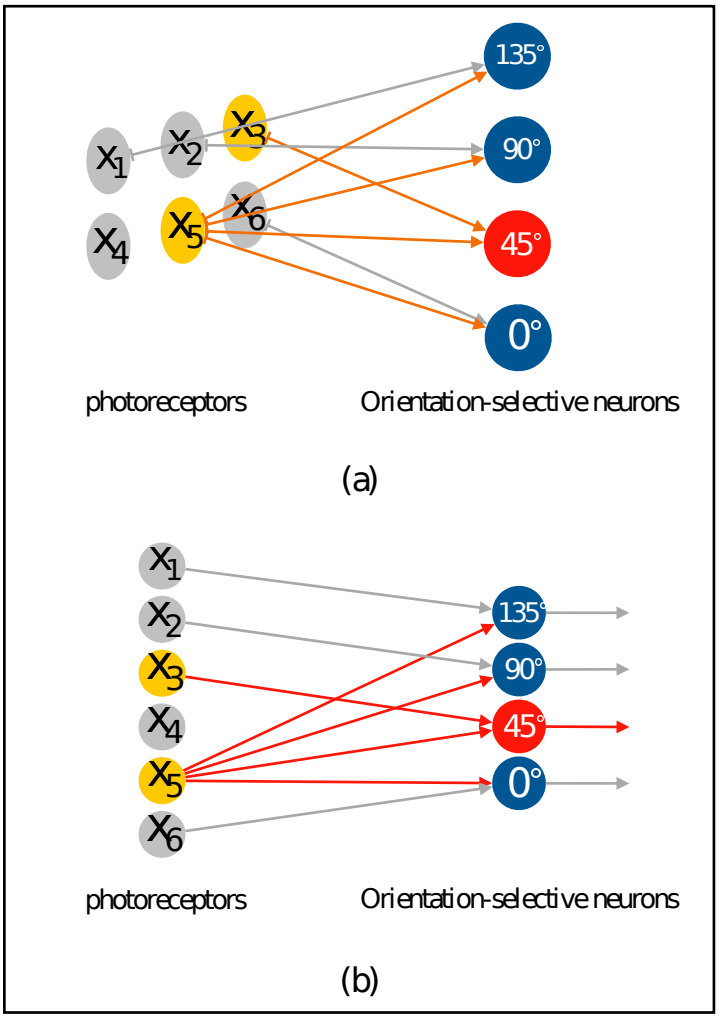

Figure 3.3: The neural connections in a local receptive field. (a) The connections between photoreceptors and orientation-selective neurons, (b) the perceptron form of the connections between photoreceptors and orientation-selective neurons.

3.3 Global Orientation Detection System

In this subsection, we describe the entire global detection process of the single-layer perceptron AVS for orientation detection. The system for two-dimensional global orientation detection can be expressed in Figure 3.4. Take an object which is 135° in orientation as an example. In Figure 3.4, the positions of corresponding photoreceptors activated by this object are shown. The photoreceptors which received light are colored yellow; others colored gray. This image with 5×4 regions can be divided into 9 independent local receptive fields

of 3×2 size. Then the photoreceptors in each local receptive field are connected to the four different orientation-selective neurons. So, there are a total of 36 orientation-selective neurons connected to the photoreceptors for this 5×4 image. Three local receptive fields and their corresponding orientation-selective neurons are shown in the figure. The three local regions are shown in colored frames. Activated orientation-selective neurons are colored red, and inactivated orientation-selective neurons are colored blue. In one orientation detection process, the inputs in each local receptive field are transmitted into four orientation-selective neurons. And the local orientation information is computed respectively by the four types of orientation-selective neurons.

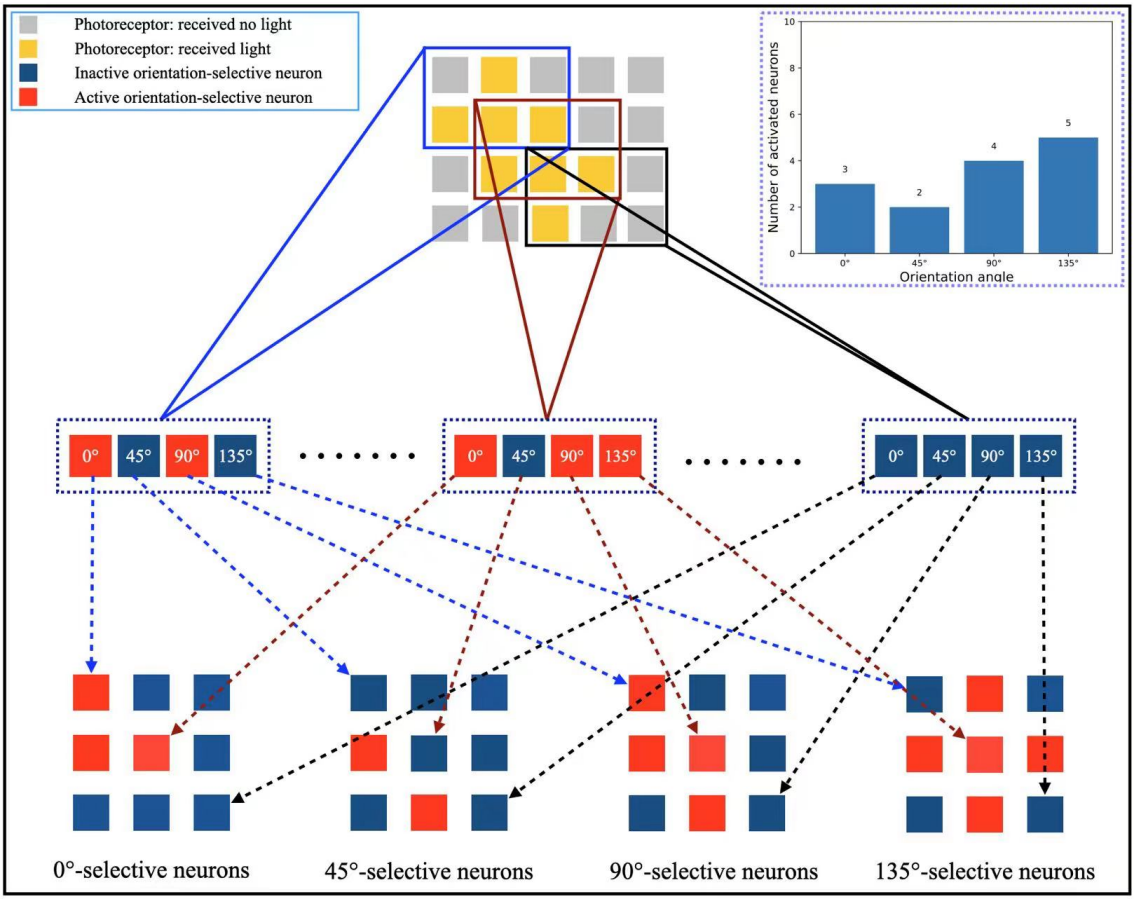

Figure 3.4: The mechanism of the perceptron AVS for two-dimensional global orientation detection.

The corresponding orientation-selective neurons are activated according to the effective

local orientation information. For example, the inputs in the first local receptive field only activate a 0°-selective neuron and a 90°-selective neuron. The inputs in the last local receptive field activate no neurons. When we arrange the orientation-selective neurons according to the corresponding positions, the arrangements are shown at the bottom part of Figure 3.4. We can easily know the corresponding positions of activated neurons and the number of different types of activated neurons. The activations of four types of orientation-selective neurons are shown in the bar chart. Because the global orientation can be obtained according to the number of orientation-selective neurons most activated, the type of neurons with the most activations corresponds to the global orientation of the object. From the bar chart, we can know that five 135°-selective neurons are activated 5 times, which is activated most. So the detection result is that this object is 135° in orientation.

The whole system for two-dimensional global orientation detection based on single-layer perceptron is shown in Figure 3.5. It consists of three layers: photoreceptor layer, local orientation-selective neuron layer and sum layer. From the photoreceptor layer to the local orientation-selective neuron layer, they are not fully connected. Each local orientation-selective neuron accepts specific inputs. According to the distribution characteristics of different input groups in the local receptive field, neurons can be defined as four different orientation-selective neurons. Finally, the outputs from the same type of local orientation-selective neurons are sent to a summer, and simple summed in the summer layer. This step is for calculating the sum of effective inputs, that is, to count the number of this type of neuron activated. So the four final output results are the numbers of four kinds of neurons activated. In this system, effective connections and active neurons are colored red. The active neuron's output value is 1, and the inactive neuron's output value is 0. The four results are consistent with the results shown in Figure 3.4.

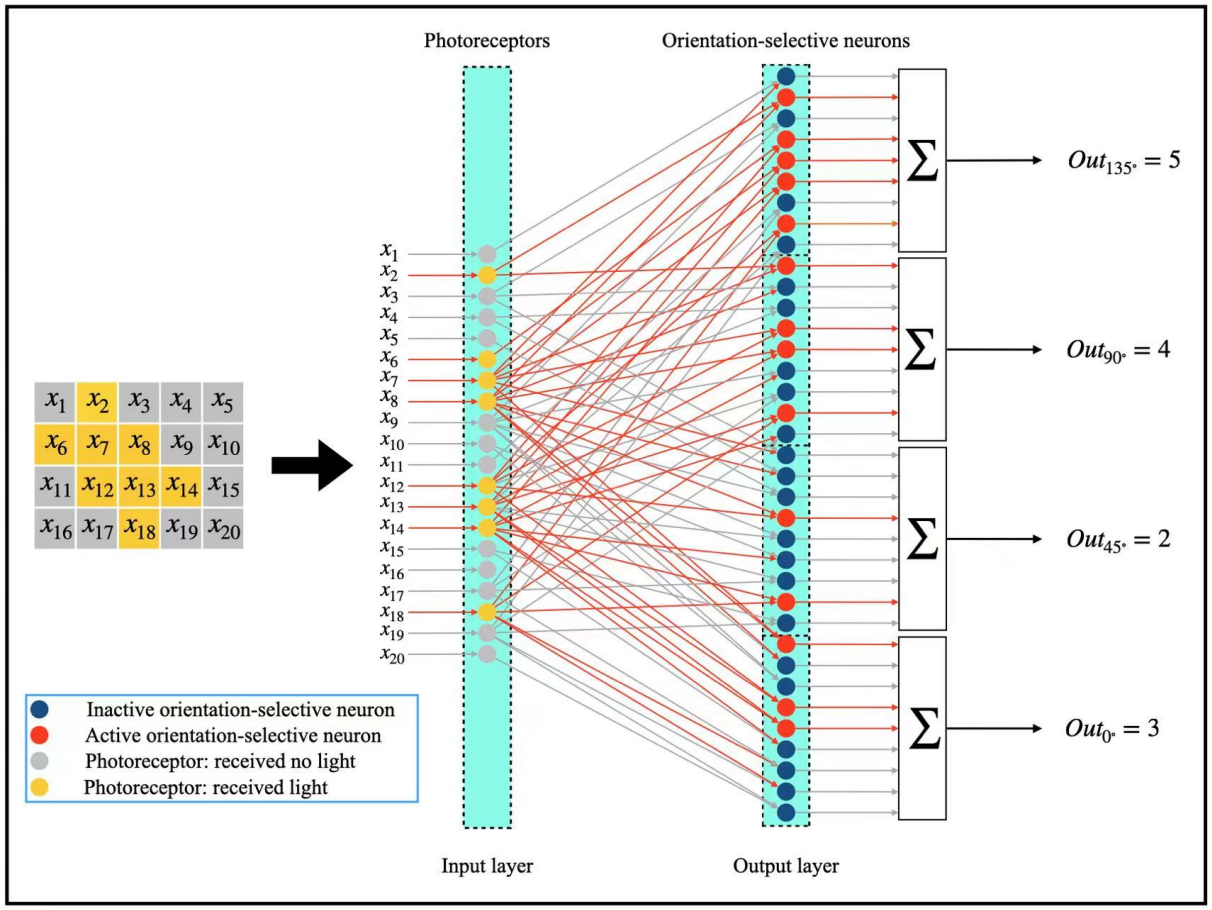

Figure 3.5: The single-layer perceptron AVS for two-dimensional global orientation detection.

3.4 Simulation Result

To validate the single-layer perceptron AVS for global orientation detection, we conducted several computer experiments. We generated a dataset that consisted of 49,694 binary images. All images were sized to 1024 pixels (32×32), and each image had different numbers of light spots arranged into a regular object with central symmetry or axial symmetry in one specific orientation angle. For orientation detection of an object in each image, we applied four different orientation-selective neurons to each local receptive field for local orientation detection, and used the numbers of activation of each type of neurons to infer global orientation. Considering the edge information and the size of each local receptive field of 3×2, for each 32×32 image, we padded 0 values on the boundary of the image matrix (right, left and up). After padding, the size of one image became to 34×33 so that it can be divided into 1024 (32×32) local receptive fields. Consequently, a total of 4096 (4×1024) orientation-selective neurons were required to participate in orientation detection. In the first experiment, we placed a line of 1×10 to a 135° orientation, as shown in Figure 3.6(a), applied it to the 4 types of totally 4096 orientation-selective neurons and recorded the activations of the 4 types of orientation-selective neurons (overall activations (in Figure 3.6(b)) and individual activations of 0°-selective neurons, 45°-selective neurons, 90°-selective neurons and 135°-selective neurons (Figure 3.6(c)). As can be seen from Figure 3.6(b) and (c), only the 135° orientation-selective neuron was activated, whereas other orientation-selective neurons were not activated. Thus, the orientation-sensitive neuron (135°) with the largest number of activations can be used as the global orientation of the line. We also changed the lengths, angles and positions of the line and found that although the lengths, angles and positions of the activated 135°-sensitive neuron were different, only the 135° orientation-sensitive neuron was activated. Next, we used a 135° 4×10 pixel bar as the stimulus (Figure 3.7(a)), applied it to the 4 types of totally 4096 orientation-selective neurons and recorded the activations of the 4 types of orientation-selective neurons (overall activations

(Figure 3.7(b)) and individual activations of 0°-selective neurons, 45°-selective neurons, 90°-selective neurons and 135°-selective neurons (Figure 3.7(c)). It is very interesting to note that there were 28 0°-selective neurons, 20 45°-selective neurons, 29 90°-selective neurons and 36 135°-selective neurons activated to the 135° 4×10 pixel bar. From this, we can also correctly judge that the bar was placed in 135° orientation. Furthermore, we also changed the lengths, widths, angles and positions of the bar and found that although the lengths, widths, angles, positions and the number of the activated 0°-selective neurons, 45°-selective neurons, 90°-selective neurons and 135°-selective neurons were different, 135°-sensitive neurons fired most. The above experiments captured key experimental observations [51], might provide explanations for these experimental observations, and lead neuroanatomists and neurophysiologists to reexamine their observations or redesign their experiments.

3.5 Conclusion and Disscasion

In this chapter, we proposed a novel orientation detection mechanism based single-perceptron AVS. Considering that neurons can only perform simple neural computation, we assumed that there are neurons that can only detect a specific orientation of an object locally. We introduced the idea of the local receptive field into our mechanism, and each local information is collected by an individual local orientation detective neuron. According to the numbers of activated orientation detective neurons, the global orientation angle of the object was determined by the most activated orientation detective neuron. We implemented the global orientation detection system with a single-layer perceptron and have proved the effectiveness of the system through a large number of computer experiments. The experimental results showed its excellent recognition accuracy regardless of the size, location and orientation of objects.

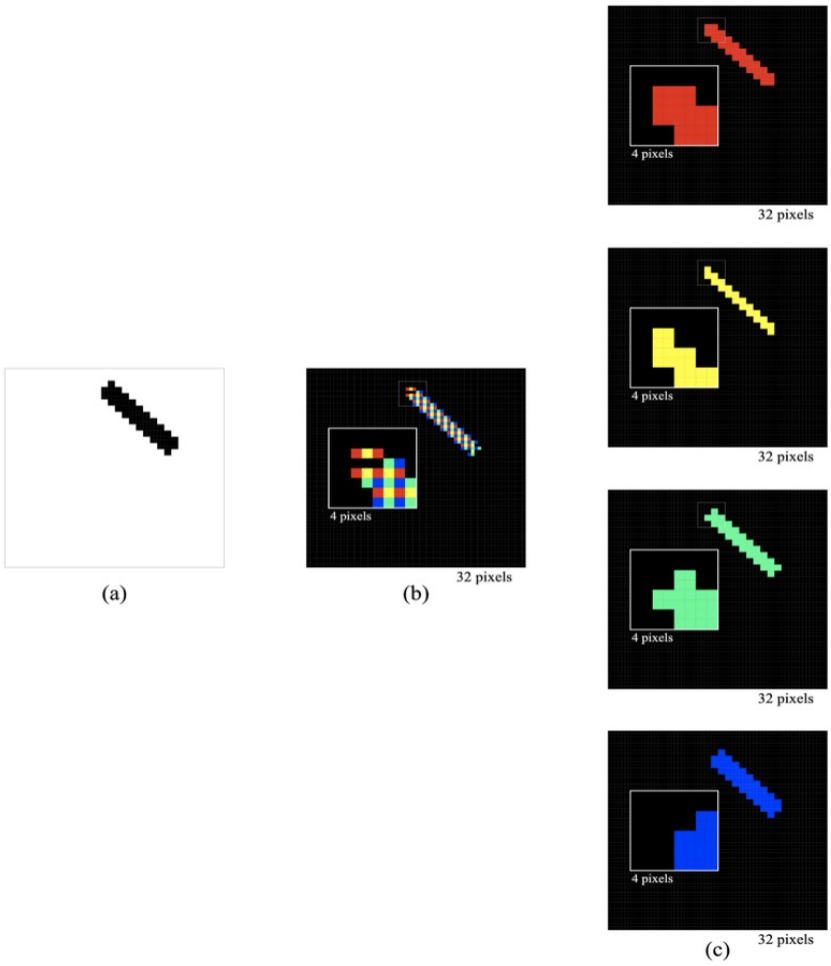

Figure 3.6: Simulated responses of the local orientation detective neurons to a line stimulus of at a orientation (a), overall activations (b) and individual activations of -selective neurons, -selective neurons, -selective neurons and -selective neurons (c).

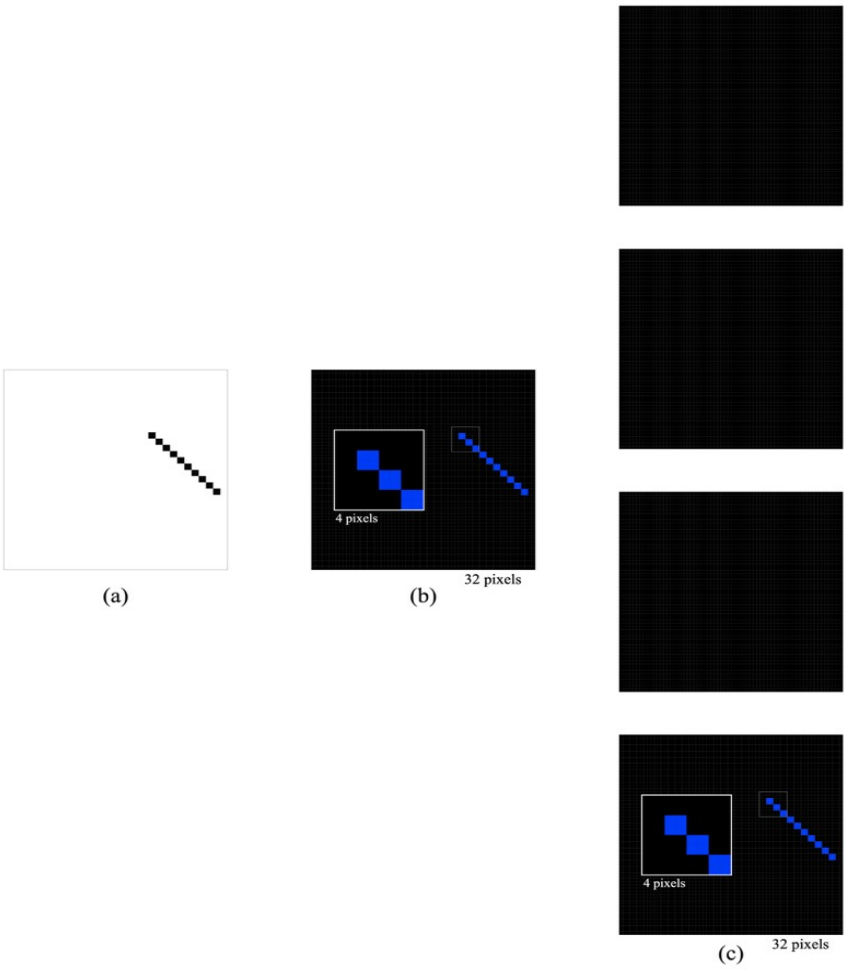

Figure 3.7: Simulated responses of the local orientation detective neurons to a bar stimulus of at a orientation (a), overall activations (b) and individual activations of -selective neurons, -selective neurons, -selective neurons and -selective neurons (c).

Chapter 4

Learning Algorithm with Advanced Learning Strategy

4.1 Teaching-Learning-Based Optimization (TLBO)

TLBO is a nature-inspired optimization method inspired by the influence of teachers on learners [67]. TLBO is similar to other nature-inspired algorithms that uses populations to proceed to the global optimal solution. Each learner is considered as an individual of populations. The grade of learner is analogous to the fitness, and learner who has the best fitness in each iteration is considered as teacher. TLBO algorithm is divided into two parts which consist of 'learner phase' and 'teacher phase', respectively. Teacher phase means that learners obtain knowledge from teacher, and the updating unit can be represented as Eq.(4.1):

$$X_i^{new} = X_i^{old} + r_i(X_{teacher} - T_F \cdot Mean) \tag{4.1}$$

where X_i indicates ith individual of population, r is a random real number between 0 and 1. T_F can be either 1 or 2 as a scaling factor. $Mean$ denotes the mathematical expectation which is calculated by the arithmetic mean of individual in population. The process of learner phase can be roughly expressed as learning through the interaction between learners. TLBO will proceed to a selection strategy through X_i and X_j which are selected from population. The learner learns something new from the other learner who has better fitness,

and this procedure can be represented as Eq. (4.2):

$$X_{new} = \begin{cases} X_i + r(X_i - X_j), if\ f(X_i) < f(X_j) \\ X_i + r(X_j - X_i), \qquad else \end{cases} \tag{4.2}$$

where $f()$ denotes the fitness of individual in population.

4.2 Global Optimum-based Search Strategy

To improve the capacity of local refinement in meta-heuristic algorithm, global optimum-based search strategy (GoS) is introduced. The aim of GoS is clear that it will break the current state of population when algorithm sticks into stagnation, as long as an individual with better fitness is found. GoS will shut down and the main optimization method proceed. The procedure of GoS can be roughly divided into two parts. One is the counter of dead time, the other is an operation when algorithm sticks into a stagnation. The implementation and equations of GoS can be expressed as Algorithm 1.

Algorithm 1 Pseudo code of GoS

```
In each iteration t
for each individual i
if X^best(t) − X^best(t − 1) then
    l(t) = l(t − 1) + 1
end if
if l(t) > L then
    X_i^new = X_i^old + (rand − 0.5) · (X_i^old − X^best)
    l(t) = 0
end if
```

In Algorithm 1, $l(\cdot)$ are the times of stagnation in an iteration, and L is a certain threshold value. Local refinement usually wastes a substantial number of function evaluation (NFEs), but GoS doesn't cost additional NFEs. GoS will only proceed when the whole population traps into local optima, the global search method will be continued after finding a better individual.

Algorithm 2 Pseudo code of ITLBO

/*Initialization*/
for $i = 1$ *to* M **do**
  randomly initialize individual X_i
  $f(X_i)$ = evaluate X_i
end for
repeat
  Select teacher $X_{teacher}$ from population
  /*Teacher phase*/
  for $i = 1$ *to* M **do**
    $X_i^{new} = X_i + r_i(X_{teacher} - T_F \cdot Mean)$
    $f(X_i^{new})$ = evaluate X_i^{new}
    if $f(X_i^{new}) < f(X_i)$ **then**
      $X_i = X_i^{new}$
    end if
    if $f(X_i^{new}) < f(X_{teacher})$ **then**
      $best = i$
    end if
  end for
  for $i = 1$ *to* M **do**
    if statisfy the condition of stagnation **then**
      /*GoS*/
      $X_i^{new} = X_i + (rand - 0.5) * (X_i - X_{best})$
    else
      /*Learner phase*/
      randomly select an individual X_j from population
      if $f(X_i) < f(X_j)$ **then**
        $X_i^{new} = X_i + rand * (X_i - X_j)$
      else
        $X_i^{new} = X_i + rand * (X_j - X_i)$
      end if
    end if
    $f(X_i^{new})$ = evaluate X_i^{new}
    if $f(X_i^{new}) < f(X_i)$ **then**
      $X_i = X_i^{new}$
    end if
  end for
until Terminal Condition

Table 4.1: Experiment results of ITLBO, TLBO, GWO and SCA on IEEE CEC2017.

	ITLBO	TLBO	GWO	NCS
	Mean ± Std	Mean ± Std	Mean ± Std	Mean ± Std
F1	2.50E+03 ± 2.49E+03	**1.58E+03** ± 2.41E+03	1.02E+09 ± 8.91E+08	9.35E+07 ± 1.22E+07
F3	**6.10E+02** ± 3.43E+02	7.03E+02 ± 3.56E+02	2.85E+04 ± 9.70E+03	6.39E+04 ± 1.14E+04
F4	**4.56E+02** ± 2.46E+01	4.68E+02 ± 3.09E+01	5.70E+02 ± 4.98E+01	5.15E+02 ± 1.81E+01
F5	**5.64E+02** ± 1.83E+01	5.69E+02 ± 1.50E+01	5.92E+02 ± 2.63E+01	8.37E+02 ± 2.98E+01
F6	6.03E+02 ± 1.72E+00	**6.02E+02** ± 2.11E+00	6.04E+02 ± 2.33E+00	6.78E+02 ± 6.01E+00
F7	**8.00E+02** ± 1.98E+01	8.03E+02 ± 2.28E+01	8.35E+02 ± 4.95E+01	1.30E+03 ± 7.44E+01
F8	**8.51E+02** ± 1.41E+01	8.57E+02 ± 1.54E+01	8.81E+02 ± 1.25E+01	1.08E+03 ± 2.23E+01
F9	**9.42E+02** ± 3.82E+01	9.83E+02 ± 1.34E+02	1.18E+03 ± 1.39E+02	1.85E+04 ± 2.41E+03
F10	7.61E+03 ± 4.50E+02	7.62E+03 ± 4.67E+02	**3.73E+03** ± 5.49E+02	4.89E+03 ± 2.32E+02
F11	**1.20E+03** ± 3.95E+01	1.23E+03 ± 5.46E+01	1.51E+03 ± 4.42E+02	1.36E+03 ± 4.70E+01
F12	3.50E+04 ± 1.65E+04	**3.31E+04** ± 2.39E+04	3.31E+07 ± 3.81E+07	1.78E+07 ± 4.20E+06
F13	**1.10E+04** ± 9.09E+03	1.86E+04 ± 1.56E+04	6.63E+06 ± 2.33E+07	2.40E+06 ± 5.67E+05
F14	5.29E+03 ± 3.45E+03	**5.25E+03** ± 3.08E+03	8.10E+04 ± 1.76E+05	1.04E+04 ± 4.75E+03
F15	**4.14E+03** ± 3.12E+03	5.24E+03 ± 4.69E+03	2.44E+05 ± 5.82E+05	2.36E+05 ± 8.69E+04
F16	**2.05E+03** ± 1.84E+02	2.12E+03 ± 2.10E+02	2.32E+03 ± 2.39E+02	2.77E+03 ± 1.67E+02
F17	**1.85E+03** ± 7.40E+01	1.90E+03 ± 9.75E+01	1.93E+03 ± 1.16E+02	2.07E+03 ± 8.93E+01
F18	2.04E+05 ± 1.28E+05	2.61E+05 ± 1.90E+05	7.75E+05 ± 1.40E+06	**1.54E+05** ± 4.83E+04
F19	**5.37E+03** ± 4.40E+03	8.27E+03 ± 6.40E+03	2.06E+05 ± 3.88E+05	9.83E+05 ± 3.62E+05
F20	**2.20E+03** ± 8.17E+01	2.20E+03 ± 8.95E+01	2.33E+03 ± 1.66E+02	2.59E+03 ± 1.04E+02
F21	2.35E+03 ± 1.83E+01	2.36E+03 ± 1.45E+01	2.37E+03 ± 1.85E+01	**2.29E+03** ± 1.38E+02
F22	**2.30E+03** ± 1.95E+00	2.30E+03 ± 1.89E+00	4.47E+03 ± 1.45E+03	2.53E+03 ± 7.39E+02
F23	**2.72E+03** ± 1.56E+01	2.73E+03 ± 2.18E+01	2.73E+03 ± 3.04E+01	2.95E+03 ± 1.25E+02
F24	**2.88E+03** ± 1.63E+01	2.88E+03 ± 1.64E+01	2.90E+03 ± 4.70E+01	2.92E+03 ± 2.94E+02
F25	**2.90E+03** ± 1.66E+01	2.91E+03 ± 2.13E+01	2.96E+03 ± 2.69E+01	2.92E+03 ± 1.54E+01
F26	4.35E+03 ± 7.56E+02	4.16E+03 ± 8.10E+02	4.43E+03 ± 2.45E+02	**3.01E+03** ± 1.03E+02
F27	**3.22E+03** ± 1.36E+01	3.23E+03 ± 1.92E+01	3.23E+03 ± 1.78E+01	3.29E+03 ± 2.03E+01
F28	3.17E+03 ± 5.75E+01	**3.16E+03** ± 5.42E+01	3.33E+03 ± 4.83E+01	3.27E+03 ± 2.00E+01
F29	**3.54E+03** ± 1.09E+02	3.58E+03 ± 1.18E+02	3.71E+03 ± 1.26E+02	4.18E+03 ± 8.86E+01
F30	**7.16E+03** ± 1.97E+03	7.30E+03 ± 1.39E+03	3.90E+06 ± 3.10E+06	1.80E+06 ± 4.41E+05

4.3 Hybrid Algori ITLBO

A. Motivation

It is well-known that improving the balance between exploitation and exploration is an effective way to boost performance of algorithm [23, 86]. Like most of nature-inspired metaheuristic algorithms, the search procedure of TLBO is also from decentralization to centralization. In other words, the search space of whole population will gradually focus on a promising individual, even if it is a local optima. As in 'teacher phase' of TLBO, each learner will tend to teacher. Once algorithm traps into local optima, the following searches will get half of the results with twice effort, which means that TLBO lacks of

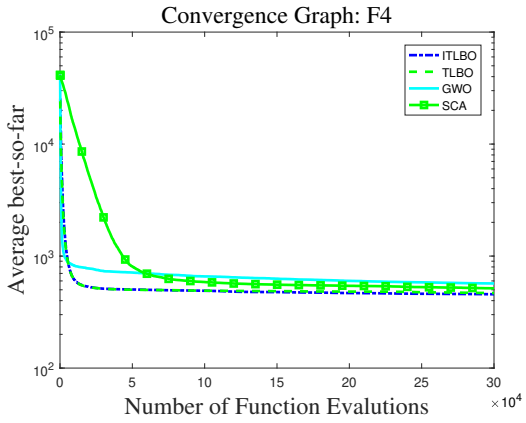

Figure 4.1: Convergence graph of F4.

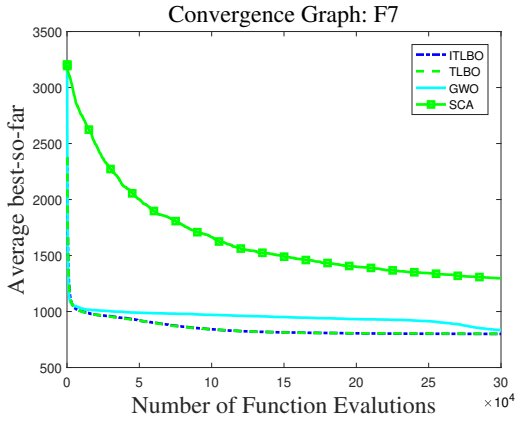

Figure 4.2: Convergence graph of F7.

exploration capacity. On the other hand, GoS has ability to break and reconstruct the state of population when the search is stagnant. In order to better balance exploration and exploitation of TLBO, we incorporates GoS into TLBO and propose a new hybrid algorithm, namely Improved Teaching-Learning-based Optimization (ITLBO).

B. The Principle of ITLBO

Based on the motivation introduced above, we aim to improve the balance between exploration and exploitation of TLBO through GoS. We utilize a new selection operation to realize the function of GoS in the learner phase, and the main steps of ITLBO is described as follows:

(1) Randomly initialize population.

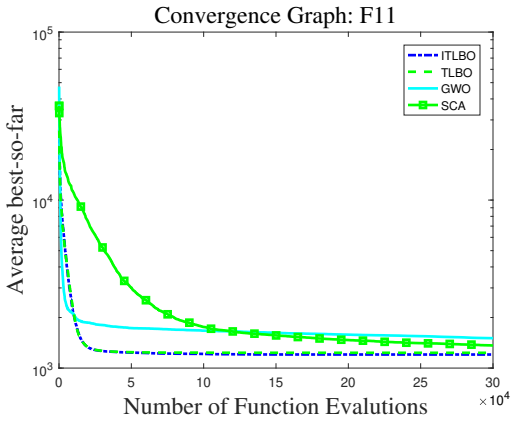

Figure 4.3: Convergence graph of F11.

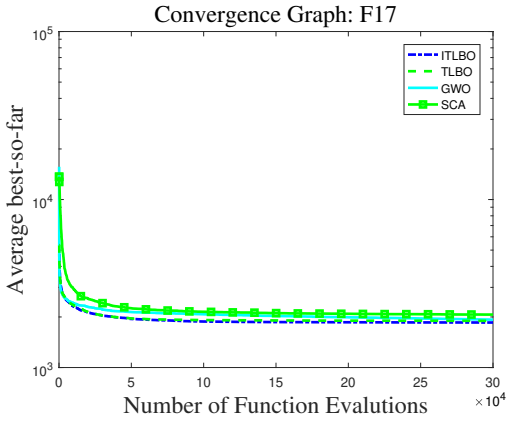

Figure 4.4: Convergence graph of F17.

(2) Evaluate the whole population, and then select best individual as teacher and calculate the mean of population.

(3) Generate the new population through Eq. (4.1), and choose the outstanding offspring into the next iteration.

(4) Judge the stagnant time of algorithm, if it exceeds the threshold value, generate new population through Eq.(4.2), otherwise, generate new population through Algorithm 1.

(5) Repeat steps(2)-(4) until fulfilling the terminal condition.

The pseudo code of ITLBO is shown as Algorithm 2, where $Mean$ denotes the arithmetic mean value of all individual in population, *best* indicates the index of best individual in current population, and it will be used in the process of GoS. The procedure of GoS is

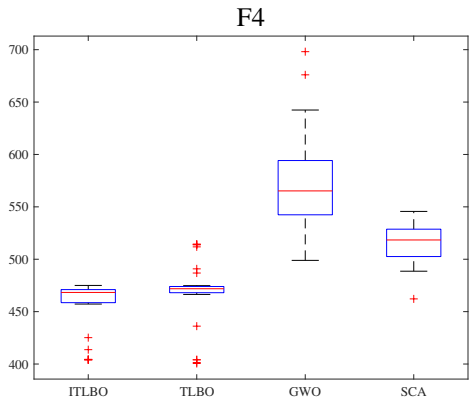

Figure 4.5: Box-and-whisker plots of of F4.

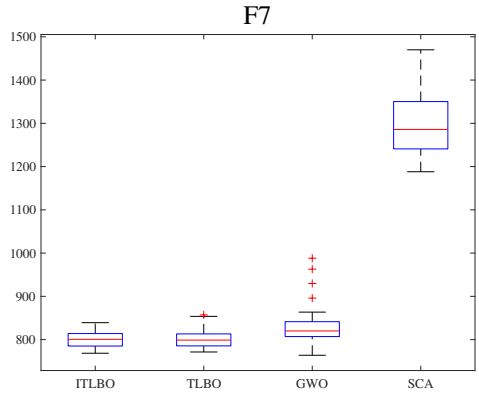

Figure 4.6: Box-and-whisker plots of of F7.

inserted into the learner phase, and condition of stagnation is described as Algorithm 1.

4.4 Experment Result

To testify the performance of the ITLBO, in addition to TLBO, ITLBO is compared with other two state-of-the-art algorithms including grey wolf optimization (GWO) [60] and sine cosine algorithm (SCA) [59]. Twenty-nine benchmark functions of IEEE CEC2017 are chosen which consists of unimodal functions (F1, F3), simple multimodal functions (F4-F10), hybrid functions (F11-F20) and complex functions (F21- F30). Each algorithm runs twenty-nine times and population size is set to 100. The maximum number of the function

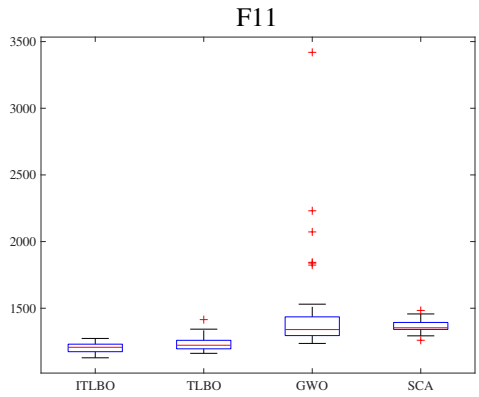

Figure 4.7: Box-and-whisker plots of of F11.

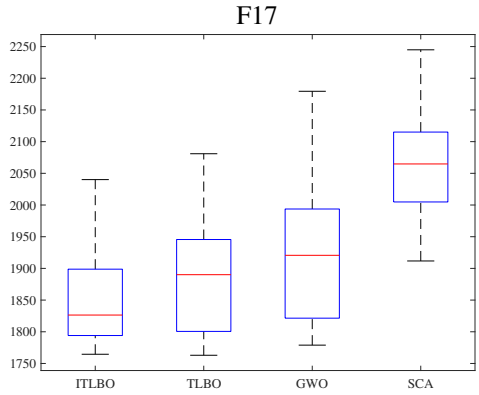

Figure 4.8: Box-and-whisker plots of of F17.

evaluations is $D * 10000$ where D indicates size of dimension. Experimental results are listed in Table 4.1, where the highlighted data are the best results among four algorithms. The other recorded results are the standard deviation between obtained function values and the known optimal value. The results of Wilcoxon matched-pairs signed-rank test are summarized in Table 4.2. The convergence graphs are shown as Figs. 4.1-4.4 and box-and-whisker graphs are exhibited in Figs. 4.5-4.8.

It is apparent that the proposed algorithm ITLBO has better performance in comparison with those state-of-the-art algorithms through Table 4.1. It is also evident that the curve slope of ITLBO is larger than two algorithms GWO and SCA in Figs. 4.1-4.4 which means the speed of convergence of ITLBO is faster. The convergence results of ITLBO outperform

Table 4.2: Results obtained by the Wilcoxon test for ITLBO.

VS	R^+	R^-	p-value
TLBO	306.5	99.5	1.73E-2
GWO	415.0	20.0	1.38E-6
NCS	372.0	63.0	4.51E-4

other algorithms, and the whole search process of ITLBO is harder to stick into stagnation, which denotes that the incorporation of GoS into TLBO is effective. The reason is that TLBO mainly provides the global search ability and GoS can break and reconstruct the state of stagnation. The balance between exploration and exploitation of ITLBO is reliable. We can conclude that ITLBO performs remarkable effectiveness and robustness on function optimization problems.

4.5 Conclusions

In this chapter, we utilize a global optimum-based search strategy GoS to promote the exploration ability of nature- inspired metaheuristic algorithm TLBO and propose a new algorithm called ITLBO. The classic TLBO has strong capacity of exploitation but difficult to break away stagnant state. To alleviate this issue, we set a threshold by which the algorithm will execute GoS when dead time of global search exceed the threshold, while the main procedure of TLBO will proceed once a better individual is found. To verify the performance of proposed algorithm, we compared it with TLBO, GWO, SCA based on twenty-nine benchmark functions of IEEE CEC2017. Experimental results prove the effectiveness and robustness of ITLBO in comparison with other state-of-the-art algorithm. In the future, we will focus on solving some real-world problems via ITLBO, such as Internet of vehicles [85]– [88], dynamic location routing problem, artificial neural network learning problems [24, 40, 42, 78], time-series prediction [84, 96], and protein structure prediction [19, 74].

Chapter 5

Conclusions

This paper described a mechanism for detecting the global orientation by introducing local orientation detective neurons to compute local orientation, and schemes to judge global orientation from these local orientation information. We assumed that neurons, we call them the local orientation detective neurons, exist in visual nervous system. Each of the local orientation detective neurons receives its own input through photoreceptor and ON-OFF cells from receptive field, picks up selectively an adjacent input, and computes to response only to the orientation from the selected adjacent input. That is to say that within local receptive field, the local orientation detective neurons can extract elementary visual feature such as orientation. These features are then combined by the subsequent layers in order to detect higher-order feature, for example, the global orientation.

Furthermore, we proposed two implementations of the local orientation detective neurons. First, we implemented the local orientation detective neuron based on the dendritic neuron model that authors proposed previously and extend it to several orientation detective neurons that response only to their own particular orientation. Secondly, we used the single-layer perceptron to realize the local orientation detective neurons. Then, we proposed four possible schemes to measure the activations of the local orientation detective neurons: (1) scanning over a two-dimensional inputs of an image, for every inputs, convolving their adjacent inputs with a local orientation detective neuron; (2) scanning over a two-dimensional inputs of an image with a group of the local orientation detective neurons,

(3) sliding over a two-dimensional inputs of an image with a small array of a grouped local orientation detective neurons and (4) making a two-dimensional inputs of an image follow their own local orientation detective neurons independently. Since these neurons give the local motion responses that are localized in space; and these neurons' outputs can be taken as evidence about the global orientation, thus we can obtain global orientation directly by measuring the outputs of these local orientation detective neurons. We implemented the global orientation detection systems with dendritic neurons and a single-layer perceptron, respectively. We have proved the effectiveness of the systems through a large number of computer experiments. The experimental results showed their excellent recognition accuracy regardless of the size, location and orientation of objects.

Based on the mechanism, we developed an Artificial Visual System (ASV). In order to compare the performance of Artificial Visual System (ASV) and Convolutional Neural Network (CNN), we applied the Artificial Visual System (ASV) without learning and Convolutional Neural Network (CNN) with learning to the orientation detection and found that the Artificial Visual System (ASV) was completely better than the Convolutional Neural Network (CNN) in terms of accuracy and noise tolerance. Preliminary experiments of the Artificial Visual System (ASV) to the motion direction detection, motion speed detection, the perception of the binocular vision without learning, and pattern recognition with learning also showed that the Artificial Visual System (ASV) completely beaten the Convolutional Neural Network (CNN) in terms of accuracy and noise tolerance, which are reported in our next paper. Therefore we believe that the Artificial Visual System (ASV) is very likely to completely replace the Convolutional Neural Network (CNN) in near future.

In this paper, we also utilized a global optimum-based search strategy GoS to promote the exploration ability of nature-inspired metaheuristic algorithm TLBO and proposed a new algorithm called ITLBO. The classic TLBO has strong capacity of exploitation but difficult to break away stagnant state. To alleviate this issue, we set a threshold by which the algorithm will execute GoS when dead time of global search exceed the threshold, while

the main procedure of TLBO will proceed once a better individual is found. To verify the performance of proposed algorithm, we compared it with TLBO, GWO, SCA based on twenty-nine benchmark functions of IEEE CEC2017. Experimental results prove the effectiveness and robustness of ITLBO in comparison with other state-of-the-art algorithm. In the future, we will focus on solving some real-world problems via ITLBO, such as Internet of vehicles, dynamic location routing problem, artificial neural network learning problems, time-series prediction and protein structure prediction.

Bibliography

[1] Hagai Agmon-Snir, Catherine E Carr, and John Rinzel. The role of dendrites in auditory coincidence detection. *Nature*, 393(6682):268–272, 1998.

[2] Qeethara Kadhim Al-Shayea. Artificial neural networks in medical diagnosis. *International Journal of Computer Science Issues*, 8(2):150–154, 2011.

[3] James S Albus. A theory of cerebellar function. *Mathematical biosciences*, 10(1-2):25–61, 1971.

[4] JC Anderson, T Binzegger, O Kahana, KAC Martin, and I Segev. Dendritic asymmetry cannot account for directional responses of neurons in visual cortex. *Nature neuroscience*, 2(9):820–824, 1999.

[5] Alain Artola, S Bröcher, and Wolf Singer. Different voltage-dependent thresholds for inducing long-term depression and long-term potentiation in slices of rat visual cortex. *Nature*, 347(6288):69–72, 1990.

[6] Guo-qiang Bi and Mu-ming Poo. Synaptic modifications in cultured hippocampal neurons: dependence on spike timing, synaptic strength, and postsynaptic cell type. *Journal of neuroscience*, 18(24):10464–10472, 1998.

[7] Barbara Chapman, Kathleen R Zahs, and Michael P Stryker. Relation of cortical cell orientation selectivity to alignment of receptive fields of the geniculocortical afferents that arborize within a single orientation column in ferret visual cortex. *Journal of Neuroscience*, 11(5):1347–1358, 1991.

[8] Chong Chen and Susumu Tonegawa. Molecular genetic analysis of synaptic plasticity, activity-dependent neural development, learning, and memory in the mammalian brain. *Annual review of neuroscience*, 20(1):157–184, 1997.

[9] Jiujun Cheng, Minjun Chen, MengChu Zhou, Shangce Gao, Chunmei Liu, and Cong Liu. Overlapping community change-point detection in an evolving network. *IEEE Transactions on Big Data*, 6(1):189–200, 2018.

[10] JiuJun Cheng, JunLu Cheng, MengChu Zhou, FuQiang Liu, ShangCe Gao, and Cong Liu. Routing in internet of vehicles: A review. *IEEE Transactions on Intelligent Transportation Systems*, 16(5):2339–2352, 2015.

[11] Jiujun Cheng, Xiao Wu, Mengchu Zhou, Shangce Gao, Zhenhua Huang, and Cong Liu. A novel method for detecting new overlapping community in complex evolving networks. *IEEE Transactions on Systems, Man, and Cybernetics: Systems*, 49(9):1832–1844, 2018.

[12] Jiujun Cheng, Guiyuan Yuan, MengChu Zhou, Shangce Gao, Cong Liu, and Hua Duan. A fluid mechanics-based data flow model to estimate vanet capacity. *IEEE Transactions on Intelligent Transportation Systems*, 21(6):2603–2614, 2019.

[13] Hongwei Dai, Yu Yang, Cunhua Li, Jun Shi, Shangce Gao, and Zheng Tang. Quantum interference crossover-based clonal selection algorithm and its application to traveling salesman problem. *IEICE TRANSACTIONS on Information and Systems*, 92(1):78–85, 2009.

[14] Hans C Dringenberg, Bana Hamze, Amanda Wilson, William Speechley, and Min-Ching Kuo. Heterosynaptic facilitation of in vivo thalamocortical long-term potentiation in the adult rat visual cortex by acetylcholine. *Cerebral Cortex*, 17(4):839–848, 2007.

[15] Andries P Engelbrecht. *Computational intelligence: an introduction*. John Wiley & Sons, 2007.

[16] Thomas Euler, Peter B Detwiler, and Winfried Denk. Directionally selective calcium signals in dendrites of starburst amacrine cells. *Nature*, 418(6900):845–852, 2002.

[17] Pierre A Fortier and Chelsea Bray. Influence of asymmetric attenuation of single and paired dendritic inputs on summation of synaptic potentials and initiation of action potentials. *Neuroscience*, 236:195–209, 2013.

[18] Shelley I Fried, Thomas A Münch, and Frank S Werblin. Mechanisms and circuitry underlying directional selectivity in the retina. *Nature*, 420(6914):411–414, 2002.

[19] Shangce Gao, Shuangbao Song, Jiujun Cheng, Yuki Todo, and Mengchu Zhou. Incorporation of solvent effect into multi-objective evolutionary algorithm for improved protein structure prediction. *IEEE/ACM transactions on computational biology and bioinformatics*, 15(4):1365–1378, 2017.

[20] Shangce Gao, Zheng Tang, Hongwei Dai, and Jianchen Zhang. An improved clonal selection algorithm and its application to traveling salesman problems. *IEICE transactions on fundamentals of electronics, communications and computer sciences*, 90(12):2930–2938, 2007.

[21] Shangce Gao, Wei Wang, Hongwei Dai, Fangjia Li, and Zheng Tang. Improved clonal selection algorithm combined with ant colony optimization. *IEICE transactions on information and systems*, 91(6):1813–1823, 2008.

[22] Shangce Gao, Yirui Wang, Jiujun Cheng, Yasuhiro Inazumi, and Zheng Tang. Ant colony optimization with clustering for solving the dynamic location routing problem. *Applied Mathematics and Computation*, 285:149–173, 2016.

[23] Shangce Gao, Yang Yu, Yirui Wang, Jiahai Wang, Jiujun Cheng, and MengChu Zhou. Chaotic local search-based differential evolution algorithms for optimization. *IEEE Transactions on Systems, Man, and Cybernetics: Systems*, 51(6):3954–3967, 2019.

[24] Shangce Gao, Mengchu Zhou, Yirui Wang, Jiujun Cheng, Hanaki Yachi, and Jiahai Wang. Dendritic neuron model with effective learning algorithms for classification, approximation, and prediction. *IEEE transactions on neural networks and learning systems*, 30(2):601–614, 2018.

[25] Wulfram Gerstner, Richard Kempter, J Leo Van Hemmen, and Hermann Wagner. A neuronal learning rule for sub-millisecond temporal coding. *Nature*, 383(6595):76–78, 1996.

[26] Albert Gidon, Timothy Adam Zolnik, Pawel Fidzinski, Felix Bolduan, Athanasia Papoutsi, Panayiota Poirazi, Martin Holtkamp, Imre Vida, and Matthew Evan Larkum. Dendritic action potentials and computation in human layer 2/3 cortical neurons. *Science*, 367(6473):83–87, 2020.

[27] Charles D Gilbert and Wu Li. Adult visual cortical plasticity. *Neuron*, 75(2):250–264, 2012.

[28] Nace L Golding and Nelson Spruston. Dendritic sodium spikes are variable triggers of axonal action potentials in hippocampal ca1 pyramidal neurons. *Neuron*, 21(5):1189–1200, 1998.

[29] Erkam Guresen, Gulgun Kayakutlu, and Tugrul U Daim. Using artificial neural network models in stock market index prediction. *Expert Systems with Applications*, 38(8):10389–10397, 2011.

[30] Mohamad H Hassoun et al. *Fundamentals of artificial neural networks*. MIT press, 1995.

[31] Michael Hausser, Nelson Spruston, and Greg J Stuart. Diversity and dynamics of dendritic signaling. *Science*, 290(5492):739–744, 2000.

[32] Donald Olding Hebb. *The organization of behavior: A neuropsychological theory*. Psychology Press, 2005.

[33] Anthony Holtmaat and Karel Svoboda. Experience-dependent structural synaptic plasticity in the mammalian brain. *Nature Reviews Neuroscience*, 10(9):647–658, 2009.

[34] Kuo-lin Hsu, Hoshin Vijai Gupta, and Soroosh Sorooshian. Artificial neural network modeling of the rainfall-runoff process. *Water resources research*, 31(10):2517–2530, 1995.

[35] David H Hubel and Torsten N Wiesel. Receptive fields of single neurones in the cat's striate cortex. *The Journal of physiology*, 148(3):574, 1959.

[36] David H Hubel and Torsten N Wiesel. Receptive fields, binocular interaction and functional architecture in the cat's visual cortex. *The Journal of physiology*, 160(1):106, 1962.

[37] Masao Ito, Masaki Sakurai, and Pavich Tongroach. Climbing fibre induced depression of both mossy fibre responsiveness and glutamate sensitivity of cerebellar purkinje cells. *The Journal of physiology*, 324(1):113–134, 1982.

[38] Junkai Ji, Shangce Gao, Jiujun Cheng, Zheng Tang, and Yuki Todo. An approximate logic neuron model with a dendritic structure. *Neurocomputing*, 173:1775–1783, 2016.

[39] Junkai Ji, Shuangbao Song, Cheng Tang, Shangce Gao, Zheng Tang, and Yuki Todo. An artificial bee colony algorithm search guided by scale-free networks. *Information Sciences*, 473:142–165, 2019.

[40] Junkai Ji, Shuangbao Song, Yajiao Tang, Shangce Gao, Zheng Tang, and Yuki Todo. Approximate logic neuron model trained by states of matter search algorithm. *Knowledge-Based Systems*, 163:120–130, 2019.

[41] Tao Jiang, Shangce Gao, Dizhou Wang, Junkai Ji, Yuki Todo, and Zheng Tang. A neuron model with synaptic nonlinearities in a dendritic tree for liver disorders. *IEEJ Transactions on Electrical and Electronic Engineering*, 12(1):105–115, 2017.

[42] Tao Jiang, Shangce Gao, Dizhou Wang, Junkai Ji, Yuki Todo, and Zheng Tang. A neuron model with synaptic nonlinearities in a dendritic tree for liver disorders. *IEEJ Transactions on Electrical and Electronic Engineering*, 12(1):105–115, 2017.

[43] Jianzhong Jin, Yushi Wang, Harvey A Swadlow, and Jose M Alonso. Population receptive fields of on and off thalamic inputs to an orientation column in visual cortex. *Nature neuroscience*, 14(2):232–238, 2011.

[44] Eric R Kandel, James H Schwartz, Thomas M Jessell, Steven Siegelbaum, A James Hudspeth, Sarah Mack, et al. *Principles of neural science*, volume 4. McGraw-hill New York, 2000.

[45] Dervis Karaboga and Bahriye Basturk. A powerful and efficient algorithm for numerical function optimization: artificial bee colony (abc) algorithm. *Journal of global optimization*, 39(3):459–471, 2007.

[46] Adam Kepecs, Xiao-Jing Wang, and John Lisman. Bursting neurons signal input slope. *Journal of Neuroscience*, 22(20):9053–9062, 2002.

[47] Mehdi Khashei and Mehdi Bijari. An artificial neural network (p, d, q) model for timeseries forecasting. *Expert Systems with applications*, 37(1):479–489, 2010.

[48] Christof Koch. *Biophysics of computation: information processing in single neurons*. Oxford university press, 2004.

[49] Christof Koch, Tomaso Poggio, and Vincent Torre. Retinal ganglion cells: a functional interpretation of dendritic morphology. *Philosophical Transactions of the Royal Society of London. B, Biological Sciences*, 298(1090):227–263, 1982.

[50] Christof Koch, Tomaso Poggio, and Vincent Torre. Nonlinear interactions in a dendritic tree: localization, timing, and role in information processing. *Proceedings of the National Academy of Sciences*, 80(9):2799–2802, 1983.

[51] Satoru Kondo, Takashi Yoshida, and Kenichi Ohki. Mixed functional microarchitectures for orientation selectivity in the mouse primary visual cortex. *Nature communications*, 7(1):1–16, 2016.

[52] Yann LeCun, Léon Bottou, Yoshua Bengio, and Patrick Haffner. Gradient-based learning applied to document recognition. *Proceedings of the IEEE*, 86(11):2278–2324, 1998.

[53] Michael London and Michael Häusser. Dendritic computation. *Annu. Rev. Neurosci.*, 28:503–532, 2005.

[54] Jeffrey C Magee. Dendritic integration of excitatory synaptic input. *Nature Reviews Neuroscience*, 1(3):181–190, 2000.

[55] David Marr and W Thomas Thach. A theory of cerebellar cortex. In *From the Retina to the Neocortex*, pages 11–50. Springer, 1991.

[56] Marco Martina, Imre Vida, and Peter Jonas. Distal initiation and active propagation of action potentials in interneuron dendrites. *Science*, 287(5451):295–300, 2000.

[57] Warren S McCulloch and Walter Pitts. A logical calculus of the ideas immanent in nervous activity. *The bulletin of mathematical biophysics*, 5(4):115–133, 1943.

[58] David McLaughlin, Robert Shapley, Michael Shelley, and Dingeman J Wielaard. A neuronal network model of macaque primary visual cortex (v1): Orientation selectivity and dynamics in the input layer 4cα. *Proceedings of the National Academy of Sciences*, 97(14):8087–8092, 2000.

[59] Seyedali Mirjalili. Sca: a sine cosine algorithm for solving optimization problems. *Knowledge-based systems*, 96:120–133, 2016.

[60] Seyedali Mirjalili, Seyed Mohammad Mirjalili, and Andrew Lewis. Grey wolf optimizer. *Advances in engineering software*, 69:46–61, 2014.

[61] Michael A Nielsen. *Neural networks and deep learning*, volume 25. Determination press San Francisco, CA, USA, 2015.

[62] Albert B Novikoff. On convergence proofs for perceptrons. Technical report, STANFORD RESEARCH INST MENLO PARK CA, 1963.

[63] Nicholas Oesch, Thomas Euler, and W Rowland Taylor. Direction-selective dendritic action potentials in rabbit retina. *Neuron*, 47(5):739–750, 2005.

[64] Matteo Poggi and Stefano Mattoccia. Learning from scratch a confidence measure. In *Bmvc*, volume 2, page 4, 2016.

[65] Panayiota Poirazi, Terrence Brannon, and Bartlett W Mel. Pyramidal neuron as two-layer neural network. *Neuron*, 37(6):989–999, 2003.

[66] Nicholas J Priebe and David Ferster. Mechanisms of neuronal computation in mammalian visual cortex. *Neuron*, 75(2):194–208, 2012.

[67] R Venkata Rao, Vimal J Savsani, and DP Vakharia. Teaching–learning-based optimization: a novel method for constrained mechanical design optimization problems. *Computer-aided design*, 43(3):303–315, 2011.

[68] Frank Rosenblatt. The perceptron: a probabilistic model for information storage and organization in the brain. *Psychological review*, 65(6):386, 1958.

[69] Peter C Schwindt and Wayne E Crill. Local and propagated dendritic action potentials evoked by glutamate iontophoresis on rat neocortical pyramidal neurons. *Journal of Neurophysiology*, 77(5):2466–2483, 1997.

[70] Idan Segev and Wilfrid Rall. Excitable dendrites and spines: earlier theoretical insights elucidate recent direct observations. *Trends in neurosciences*, 21(11):453–460, 1998.

[71] Y Sekiya, T Aoyama, T Hiroki, and T Zheng. Learningpossibility that neuron model can recognize depth-rotation in threedimension. In *Proc. of 1st International Conference on Control Automation and Systems*, page 149, 2001.

[72] R Angus Silver. Neuronal arithmetic. *Nature Reviews Neuroscience*, 11(7):474–489, 2010.

[73] Sandra Single and Alexander Borst. Dendritic integration and its role in computing image velocity. *Science*, 281(5384):1848–1850, 1998.

[74] Shuangbao Song, Shangce Gao, Xingqian Chen, Dongbao Jia, Xiaoxiao Qian, and Yuki Todo. Aimoes: Archive information assisted multi-objective evolutionary strategy for ab initio protein structure prediction. *Knowledge-Based Systems*, 146:58–72, 2018.

[75] Greg Stuart, Nelson Spruston, Bert Sakmann, and Michael Häusser. Action potential initiation and backpropagation in neurons of the mammalian cns. *Trends in neurosciences*, 20(3):125–131, 1997.

[76] Greg J Stuart and Nelson Spruston. Dendritic integration: 60 years of progress. *Nature neuroscience*, 18(12):1713–1721, 2015.

[77] Deyu Tang. Spherical evolution for solving continuous optimization problems. *Applied Soft Computing*, 81:105499, 2019.

[78] Yajiao Tang, Junkai Ji, Yulin Zhu, Shangce Gao, Zheng Tang, and Yuki Todo. A differential evolution-oriented pruning neural network model for bankruptcy prediction. *Complexity*, 2019, 2019.

[79] Zheng Tang, Hiroki Tamura, Makoto Kuratu, Okihiko Ishizuka, and Koichi Tanno. A model of the neuron based on dendrite mechanisms. *Electronics and Communications in Japan (Part III: Fundamental Electronic Science)*, 84(8):11–24, 2001.

[80] W Rowland Taylor, Shigang He, William R Levick, and David I Vaney. Dendritic computation of direction selectivity by retinal ganglion cells. *Science*, 289(5488):2347–2350, 2000.

[81] W Rowland Taylor and David I Vaney. New directions in retinal research. *Trends in neurosciences*, 26(7):379–385, 2003.

[82] Yuki Todo, Hiroki Tamura, Kazuya Yamashita, and Zheng Tang. Unsupervised learnable neuron model with nonlinear interaction on dendrites. *Neural Networks*, 60:96–103, 2014.

[83] Yuki Todo, Zheng Tang, Hiroyoshi Todo, Junkai Ji, and Kazuya Yamashita. Neurons with multiplicative interactions of nonlinear synapses. *International journal of neural systems*, 29(08):1950012, 2019.

[84] Catherine Vairappan, Hiroki Tamura, Shangce Gao, and Zheng Tang. Batch type local search-based adaptive neuro-fuzzy inference system (anfis) with self-feedbacks for time-series prediction. *Neurocomputing*, 72(7-9):1870–1877, 2009.

[85] Toby J Velte and Richard H Masland. Action potentials in the dendrites of retinal ganglion cells. *Journal of neurophysiology*, 81(3):1412–1417, 1999.

[86] Jiahai Wang, Binzhong Cen, Shangce Gao, Zizhen Zhang, and Yuren Zhou. Cooperative evolutionary framework with focused search for many-objective optimization. *IEEE Transactions on Emerging Topics in Computational Intelligence*, 4(3):398–412, 2018.

[87] Wei Wang, Shangce Gao, and Zheng Tang. Improved pattern recognition with complex artificial immune system. *Soft Computing*, 13(12):1209–1217, 2009.

[88] Yirui Wang, Yang Yu, Shuyang Cao, Xingyi Zhang, and Shangce Gao. A review of applications of artificial intelligent algorithms in wind farms. *Artificial Intelligence Review*, 53(5):3447–3500, 2020.

[89] Daniel E Wilson, David E Whitney, Benjamin Scholl, and David Fitzpatrick. Orientation selectivity and the functional clustering of synaptic inputs in primary visual cortex. *Nature neuroscience*, 19(8):1003–1009, 2016.

[90] Zhe Xu, Yirui Wang, Sheng Li, Yanting Liu, Yuki Todo, and Shangce Gao. Immune algorithm combined with estimation of distribution for traveling salesman problem. *IEEJ Transactions on Electrical and Electronic Engineering*, 11:S142–S154, 2016.

[91] Santiago Ramón y Cajal. *Histologie du système nerveux de l'homme & des vertébrés: Cervelet, cerveau moyen, rétine, couche optique, corps strié, écorce cérébrale générale & régionale, grand sympathique*, volume 2. A. Maloine, 1911.

[92] Gang Yang, Junyan Yi, Shangce Gao, and Zheng Tang. An improved transiently chaotic neural network with multiple chaotic dynamics for maximum clique problem. In *Second International Conference on Innovative Computing, Informatio and Control (ICICIC 2007)*, pages 275–275. IEEE, 2007.

[93] Yang Yu, Shangce Gao, Yirui Wang, and Yuki Todo. Global optimum-based search differential evolution. *IEEE/CAA Journal of Automatica Sinica*, 6(2):379–394, 2019.

[94] Ming-Yuan Zhao, KE Tang, Gang Lu, Ming-Tian Zhou, Chong Fu, Fan Yang, and Cheng-Gong Zhang. A novel clonal selection algorithm and its application. In *2008 International Conference on Apperceiving Computing and Intelligence Analysis*, pages 385–388. IEEE, 2008.

[95] Tianle Zhou, Shangce Gao, Jiahai Wang, Chaoyi Chu, Yuki Todo, and Zheng Tang. Financial time series prediction using a dendritic neuron model. *Knowledge-Based Systems*, 105:214–224, 2016.

[96] Tianle Zhou, Shangce Gao, Jiahai Wang, Chaoyi Chu, Yuki Todo, and Zheng Tang. Financial time series prediction using a dendritic neuron model. *Knowledge-Based Systems*, 105:214–224, 2016.